DETERMINING MEAN TRANSIT TIMES OF GROUNDWATER FLOW SYSTEMS

by

Bernard Jan Stolp

A dissertation submitted to the faculty of
The University of Utah
in partial fulfillment of the requirements for the degree of

Doctor of Philosophy

in

Geology

Department of Geology and Geophysics

The University of Utah

May 2014

The University of Utah Graduate School

STATEMENT OF DISSERTATION APPROVAL

The following faculty members served as the supervisory committee chair and members for the dissertation of Bernard Jan Stolp.

Dates at right indicate the members' approval of the dissertation.

D. Kip Solomon , Chair	10-17-2013 Date Approved
Briant Kimball, Member	10-25-2013 Date Approved
John R. Bowman , Member	10-21-2013 Date Approved
Steven J. Burian , Member	10-21-2013 Date Approved
Thure E. Cerling, Member	10-17-2013 Date Approved

The dissertation has also been approved by John M. Bartley, Chair of the Department of Geology and Geophysics and by David B. Kieda, Dean of The Graduate School.

ABSTRACT

Water is the elementary component of life on Earth, and quantifying this resource is critical to understanding ecosystem viability on planetary, continental, and local scales. In a simplified partition of the Earth's freshwater resources, 75% is ice at the north and south poles, 25% is groundwater, and 0.01% exists in lakes and streams. Mean transit time is a robust description of groundwater volume within the discrete aquifers that together make up the 25% of Earth's freshwater. Mean transit time can be estimated using environmental tracer concentrations in springs and gaining streams. That is because springs and streams are locations where groundwater flow paths naturally converge. Converging flowpaths create discharge that is a flow-weighted mixture of water from the contributing aquifer. The age of that flow-weighted mixture is a good measure of the mean transit time of water as it discharges from the contributing aquifer. Mean transit time can be directly used to estimate the volume of groundwater storage in the aquifer.

Although simple in principle, there are several important topics that need to be considered when collecting and dating a broad mixture of flow paths. They include 1) the necessity for a basic conceptual perception of the investigated aquifer, 2) the non-conservative aspect of most age-dating environmental tracers once exposed to the atmosphere, and 3) the importance of estimating a transit-time distribution. These specific topics are discussed in this dissertation.

TABLE OF CONTENTS

LIST OF TABLES

LIST OF FIGURES

ACKNOWLEDGEMENTS

The National Science Foundation through award EAR-0309212 from the Hydrologic Sciences Program, the U.S. Geological Survey, and the International Atomic Energy Agency funded the work discussed in this dissertation. The landowner John Bleazard allowed access to the Sixmile System. Collaborators with fieldwork, laboratory analysis, methodology, and interpretation include Kenneth Bencala, Suzanne Bethers, Lynette Brooks, Manfred Groening, L. F. Han, Becky Hollingshaus, Terry Kenny, Briant Kimball, Upmanu Lall, Tom Marston, Melissa Masbruch, Dieter Rank, Rob Runkel, Don Semon, Lawrence Spangler, Judy Steiger, Axel Suckow, and Tomas Vitvar. The U.S. Geological Survey Toxics Program supported the sodium-bromide tracer injection and laboratory analysis. Thanks in terms of balancing work and education are extended to Pat Lambert and David Susong. Specific acknowledgement for giving me the opportunity to learn more about the timing and movement of groundwater, go to Kip Solomon. I would like to thank Colleen Delaney for understanding the enjoyment gained from curiosity and patience.

CHAPTER 1

INTRODUCTION

Sometime during 2011 human population exceeded 7,000,000,000. Ignoring all other facets, this number makes our species extremely sensitive to any alteration in the planet's biological, climatic, and hydrologic systems. Even small changes in reproduction and diversity of plants/animals, patterns/amounts of precipitation, or groundwater stored in aquifers, could have acute impact on significant numbers of people. We can no longer migrate to more favorable locations. We require resources from every location on the globe. We rely on the transport of goods across the oceans. We depend on an overall level of both social and Earth system stability.

There are a limited number of temporal and spatial datasets that describe the stability of Earth systems. They include ice cores, tree rings, quaternary geochronology, and pollen. The premise of this research is that the average age of water where it discharges or exits from the aquifer (MTT; mean transit time) is a useful description of groundwater resources. MTT represents the average time it takes for water to move from locations where the aquifer is recharged to areas where the aquifer discharges, and quantifies the relative difference between aquifer volume and the amount of actively flowing groundwater. In the extreme case where an aquifer has no active recharge or discharge, groundwater is stagnate and MTT is essentially infinite. If flow-through is relatively small compared to total volume of water stored in the aquifer, the average time

water spends in (i.e., transit time of water through) the aquifer volume is long. As flow-through increases relative to the aquifer volume, MTT decreases. The relationship between MTT, volume, and flow-through is described as: MTT = [aquifer water-volume]/[groundwater flow-through rate] (modified from *Cook and Boulke*, 2000).

The utility of MTT for groundwater-resource evaluation is that the ratio of water-volume to flow-through describes negative feedback, or stability of the flow system. Stability in this sense is the rate or pattern of change in aquifer discharge in response to changes in aquifer recharge. The implication when MTT is long is that flow-through is small relative to the aquifer volume. That creates stability because something large (aquifer volume) is altered by something small (flow-through). The stress induced by a change in flow is small and it will take a long time for the aquifer to realign to a new equilibrium. Conversely, the same flow change in a smaller volume aquifer (short MTT) represents a relatively larger stress which will be transferred across the aquifer in less time. Declines in water-levels and stream baseflow created by a 5-year drought in a groundwater resource with a 30-year MTT will take longer to manifest themselves than in a groundwater resource with a 10-year MTT.

To avoid being misinformed by aquifer characterizations embedded in MTT, there are several important attributes that need to be considered. They are 1) the qualitative natural of MTT, 2) that aquifer stability does not preclude mass balance, and 3) the differences between unconfined and confined aquifers response. Although MTT is a defined quantity, the description of groundwater-resource stability conveyed by MTT is qualitative. A system with a 30-year MTT will take longer to respond to a change in flow-through than a system with a 10-year MTT. Intuitively, the stability in the 30-year

MTT could be described as “it might take 10 to 20-years for the system to respond to a 5-year drought.” However, the 10 to 20 year timeframe is an educated guess and cannot be quantified solely on the value of the system MTT.

The second attribute is that regardless of system MTT, mass balance will be maintained. Any increase or reduction in recharge will over time result in an equal increase/reduction in system discharge. MTT addresses how an input signal is processed through the groundwater system. If recharge is reduced by 50% for 5-years, it may take 20-years for that to manifest itself in discharge, but total reduction in discharge must in due course equal the total reduction in recharge. Regardless of MTT, water is not created nor destroyed within the aquifer.

The third attribute is the flow characteristic differences in unconfined and confined aquifers. In unconfined aquifers the physical process that creates stability is draining and filling of pore space. With confined aquifers, stability is created by deformation (or strain) of the pore space caused by changes in pressure. For unconfined aquifers, aquifer-volume is the total pore-space and alteration of flow-through is related to either filling or draining of pore space. A lot of pore space and relatively small flow creates long MTT and connotes stability. In confined aquifers, aquifer volume also describes pore space. The physical process that creates buffering is not fill/drain, it is deformation (or strain) of pore space caused by changes in pressure. Pressure changes and accompanying strain propagate through aquifers more rapidly than filling and draining of pore space. However, transport velocities are for the most part independent of whether flow is unconfined or confined. As a point of review, the conceptual relationship between MTT, velocity, aquifer volume, and flow-through is ***when*** aquifer volume

increases and flow-through remains constant, ***then*** average velocity decreases and MTT increases. The bottom line is that when using MTT, an independent assessment of the degree of confinement needs to be made. A 30-year MTT in a confined aquifer does not imply the same level of stability as a 30-year MTT in an unconfined aquifer. On the other hand, a confined aquifer with a 30-year MTT does suggest more stability than a confined aquifer with a 10-year MTT.

The most effective method of determining MTT for a meaningful portion of a groundwater flow system is to collect and age-date water at locations where a broad mixture of flow paths converge. Natural convergence occurs along gaining streams and at regional springs. Stream baseflow and regional springs are often utilized for municipal water-supplies; populations depend on these discharge features for drinking water and understanding their responses is of greater consequence. Although simple in principle, there are topics that need to be considered when collecting and dating a broad mixture of flow paths. Specific issues addressed in this research include the 1) necessity for a basic conceptual perception of the investigated aquifer, 2) the nonconservative aspect of most age-dating environmental tracers once exposed to the atmosphere, and 3) the importance of estimating a transit-time distribution.

To interpret an MTT from a flow-weighted mixture of water to a reasonable estimate of the "true" MTT, it is necessary to have some conceptual understanding of aquifer processes. If a spring represents localized/focused recharge that is transported along a fault zone to a spring orifice, some concept of the flow regime is helpful in the interpretation of results. Although MTT still represents the volume to flow-through ratio, and thereby stability, a localized recharge process is likely more susceptible to alteration

(or impact) than a more spatially distributed recharge process. In the case of streams, substantial amounts of hyporheic exchange along a gaining or neutral stream reach can act to slow-down the equilibration of dissolved-gas age-dating environmental tracers to atmospheric concentrations. This is positive from a standpoint of defining MTT, and does not alter the relationship between MTT and stability. Still, it can lead to overestimating both the amount and concentration of dissolved-gas, in groundwater. Artificial persistence of dissolved-gas in stream water can also lead to over-estimating the length of a gaining stream reach and possibly the spatial extent of the aquifer contributing to streamflow. Both of these examples are given to emphasize that the methods presented cannot be blankly applied. Each hydrologic system has specific features that need to be taken into consideration.

As with the physical attributes of a groundwater system, dissolved-gas age-dating tracers are also unique when exposed to the atmosphere (i.e., as along gaining streams and surface-water originating at springs). However, all dissolved-gas concentrations change once the groundwater they are dissolved in is exposed to the atmosphere When groundwater is exposed to the atmosphere dissolved-gas concentrations begin to equilibrate with atmospheric concentrations (e.g., sulfur hexafluoride concentrations increase; helium-3 concentrations decrease). If gas exchange is rapid and the amount of groundwater inflow (or gain) to the stream or at a spring is small, surface-water will equilibrate with the atmosphere and have a “modern” age. Alternatively, if exchange is slow and inflow large, the gas signal in surface water will be representative of groundwater concentrations. The effects of gas equilibration can be reconciled by simulating gas-transport within the stream water domain. To simulate a correction for

atmospheric equilibration, the inflow and gas-exchange rates need to be measured. The likelihood of successfully correcting for equilibration can be estimated by the ratio of gas-exchange velocity to specific discharge. Rapid exchange and small amounts of groundwater inflow result in larger ratios, whereas slow exchange and large inflow create smaller ratios. The research discussed in this dissertation suggests that as the ratio approaches 15 to 20, the uncertainty in estimating MTT from stream/spring-water concentrations makes it unlikely that a meaningful quantification of MTT can be made.

If the age-dating environmental tracer is not lost by gas-exchange, then the concentration of the tracer in stream/spring water represents a weighted concentration in accordance with the amount of water transported along the flow paths that converge at the location. To convert this flow-weighted concentration to MTT, the relationship between the amounts of flow associated with each flow path needs to be established. The relationship between flow amounts and transit time is summarized by a transit-time distribution. To illustrate, consider the convergence (or mixing) of 4 hypothetical groundwater flow paths. The 1st flow path contributes 40% of the flow and is 1,000 meters (m) long. The 2nd flow path is 2,200 m long and contributes 30% of the flow; the 3rd path is 4,000 m long and contributes 20% of the flow; and the 4th flow path is 7,000 m long and contributes the remaining 10% of flow. If groundwater flow velocity is 200 meters/year (m/yr) then the transit times are 5-yr, 11-yr, 20-yr, and 35-yr. Weighting transit times by the corresponding flow percentages, the calculated MTT is 13-yr. The example illustrates how MTT is calculated when individual flow paths are characterized. In a real-world situation, there is seldom explicit information on flow amounts and age-tracer concentration for individual flow paths. The aggregated samples are collected and

a single flow-weighted age-tracer concentration is quantified. The concentration is converted to an apparent age using the appropriate age-equation. If the relationship between concentration and age (the age-equation) is linear, and the tracer input function is linear, the apparent age of the mixed sample will be the same as the MTT determined by explicitly considering the transit-time distribution (as per the hypothetical example). If the concentration/age relationship or the age-dating tracer input functions are nonlinear, the age-equation will not reproduce the MTT. The flow-weighted mean, when used in a nonlinear equation does not equate to the apparent age that is calculated when individual flow concentrations are converted to an apparent age and then flow-weighted. In the non-linear case, flow amounts and age-tracer concentrations for individual flow paths need to be assessed by assigning a theoretical transit-time distribution and adjusting the parameters of that distribution (usually MTT and/or dispersion) until a reasonable match between simulated and measured concentrations is achieved.

Choosing a transit-time distribution requires some rudimentary understanding of the spatial distribution of groundwater recharge, geometry, and confining characteristics of the aquifer system (*Cook and Bolke*, 2000, Fig. 1.2; *Bethke and Johnson*, 2002). These factors control flow-path configuration/exchange and thereby flow-path transit times. Recharge that is fairly evenly distributed across an unconfined aquifer of constant thickness tends to create a distribution of transit times similar to the hypothetical example presented in the previous paragraph. Most of the water has relatively shorter transit times and progressively less water has progressively longer transit times (commonly referred to as an exponential age model). When recharge occurs at a discrete location, such as a losing stream reach, the transit-time distribution is created mainly by dispersion along the

flow paths. Each of these examples is altered when aquifer thickness is variable and/or confining layers are present. Constraining or refining knowledge of the transit-time distribution by vertically profiling groundwater age at a single horizontal location within the aquifer (i.e., at a multiple depth completion monitoring well). The groundwater age with depth relationship determined from vertical profiling does not, however, result in a MTT. MTT is quantified from dating groundwater at a discharge location where flow paths converge at fixed horizontal locations within the aquifer system. Dispersion-dominated and exponential transit-time distributions result in unique vertical age profiles.

The development, implications, and simulation of various theoretical transit-time distributions using a lumped parameter approach are described by Malezoski and Zuber, 1983; Kirchner and others, 2000; and Sukow, 2012. The common transit-time distribution choices are piston-flow, dispersion, exponential, gamma, or some mixture. For all these distributions groundwater transit times are described with either one or two parameters, which represents a considerable simplification of the complex flow patterns that exist in most real-world aquifer systems. Nonetheless, the lumped-parameter approach is a useful first-cut method of estimating 1) aggregated aquifer characteristics, 2) transit-time distributions, and 3) the conversion of age-tracer concentrations to MTT.

A more sophisticated approach is direct simulation of flow, transport, and age-tracer concentration using finite-difference or finite-element methods (e.g., MODFLOW, MTSDMS, MODFLOW-GWT, SEAWAT, SUTRA, and OTIS). However, reliably calibrated models of flow and transport are a major undertaking that usually cannot be justified solely to interpret environmental age-tracer concentrations. However, if an existing numerical model of groundwater flow exists (constructed and calibrated for other

hydrologic assessments) it is fairly straightforward to piggy-back on a transport simulation (e.g., MT3DMS, MODFLOW-GWT, SEAWAT). These transport simulators use various forms of the advection/dispersion equation to compute transport. In these codes, porosity is the most important control on simulated transport velocity; the role of water volume and the concept of aquifer flushing are not explicitly calculated. With the confined-box model previously described, the increased MTT was simulated by increasing porosity of the confined layers to compensate for the increased water volume that is evoked by increased specific storage. This points out that for both confined and unconfined systems, the porosity values need to align with the best estimates of pore-space and compressional storage. Under confined conditions the porosity needs to be adjusted to reflect the change is storage volume created by the compressibility of water. If this is not done, the simulated transport velocity will be incorrect. Goode (1990) describes the adjustment for specific yield incorporated in MODFLOW-GWT, however, the code does not adjust for confined storage. The usual reason given for setting porosity equal to specific yield in transport simulations is lack of measured porosity data. As it turns out, porosity and specific yield plus compressional storage should be equal to ensure the concept of total water-volume, through-flow rates, and flushing are honored. Ironically, specific yield and specific storage parameters in most numerical flow simulations are sensitive to observed water-level fluctuations. Greater fluctuations force calibration to lower specific yield and storage values. Lower specific yield and storage equates to less water-volume; greater fluctuations indicate less stability. Less total water-volume decreases MTT. This supports the concept of MTT as being directly proportional to stability.

The issues of transit-time distributions and the nonconservative nature of age-tracers can be mitigated by direct sampling of groundwater. The primary reason for utilizing natural discharge locations is the convergence of a broad mixture of flow paths. A degree of that convergence can also be utilized by strategically placing shallow piezometers (or other flow path isolating sampling devices) in transverse and longitudinal transects at or along the discharge locations. Samples from the piezometers represent a subset of converging flowpaths for which the apparent ages are not as sensitive to the transit-time distribution. Gas-exchange is also not as significant in piezometer samples. These advantages are offset by the labor associated with infrastructure (device) installation, multiple sample collection/analysis, infrastructure maintenance, and the potential of missing portions of the overall flow convergence. Deeper monitoring wells, from which a vertical profile of aquifer water-volume age can be determined, are also useful. These type of wells are best placed somewhere up-gradient of natural discharge. Drilling monitoring wells through the vertical extent of an aquifer is expensive and requires significant manpower and equipment. In all cases, device sampling is not flow-weighted nor is it as simple as stream/spring-water sampling. If possible, the combination of device and stream/spring-water sampling would be the most comprehensive approach for identifying the MTT of an aquifer.

The first component of work presented in this dissertation addresses the suitability of gaining streams, specifically hyporheic exchange along Red Butte Creek, as it pertains to MTT. Red Butte Creek is located in the Wasatch Mountains directly east of Salt Lake City, Utah. The second component describes gas-exchange characteristics of the age-dating environmental tracer chloroflourocarbon-12 at the Sixmile System. The Sixmile

System is a regional spring and gaining stream located at the terminal end of the Tooele Valley groundwater basin, about 40 kilometers west of Salt Lake City, Utah. The last component describes quantification of MTT for the Fischa-Dagnitz system, which is located in the southern Vienna Basin, Austria. The transit-time distribution and effects of gas-exchange are estimated. MTT estimates are compared to an independent measure of groundwater MTT derived from a 40-year tritium time-series that exists for the system.

CHAPTER 2

HYPORHEIC TRANSIENT STORAGE EXCHANGE, TRANSIT TIME, VOLUME AND HYDRAULIC CHARACTERISTICS, RED BUTTE CREEK, UTAH

2.1 Abstract

To quantify stream/aquifer interaction and transient storage along a 4,900 meter reach of Red Butte Creek, stream discharge was measured using both tracer-dilution and area-velocity discharge measurements. The experiment was carried out in late fall 2003 when the stream was at baseflow and riparian evapotranspiration was minimal. On the basis of previous experience at similar streams, sodium bromide was injected for 50-hours, which was considered ample time for tracer to fully exchange through all transient storage zones and reach steady-state concentrations. Concentration time-series collected at 4 sites along the stream showed the expected early-time tracer breakthrough consistent with average stream velocity. However, later-time tracer concentrations slowly increased over time after initial breakthrough and clearly indicated transient conditions with respect to tracer transport. This is caused by 1) hyporheic exchange that exceeds gaged stream discharge; 2) exchange mean transit times on the order of 200 – 300-hours, and 3) a hyporheic transient storage volume that is 30-times more than the stream-channel volume. Recognizing stream-system response due to large-scale hyporheic processes prevents misinterpreting downstream tracer dilution as groundwater inflow. At Red

Butte, the results changed our concept of groundwater flow in the drainage basin. Rather than basin-scale groundwater flow, active groundwater recharge and flow appears to be limited to upper altitude areas of the basin. The pattern of exchange and extended transit times clearly illustrates that downstream transport occurs within the hyporheic zone. These conditions extend the timeframe for biogeochemical reactions as well as water availability during late summer and fall. The amount of hyporheic storage at Red Butte has the potential to extend runoff recession by several months. The "age" of hyporheic water needs to be considered when interpreting riparian evapotranspiration, system response to precipitation runoff events, and the mean transit time of groundwater in a drainage basin.

2.2 Introduction

Most water in streams originates with headwater precipitation, runoff, and springs, and is transported as open-channel flow to higher-order streams, reservoirs, and lakes. In addition to open-channel physics, water transport is also influenced by more nuanced processes of stream/aquifer interaction and transient storage. These processes are commonly quantified by looking at the spatial and temporal distribution of injected soluble, conservative tracers (i.e., stream-tracer test). When the nuances begin to dominate water transport, the implementation and interpretation of stream-tracer tests need to be modified. This paper describes those modifications as they relate to 1) tracer mass-balance, 2) concentration time-series, and 3) numerically simulating tracer transport.

To quantify stream/aquifer interaction and transient storage along 4,900 meters of Red Butte Creek, Utah, a stream-tracer test was conducted. Red Butte is an upland

catchment located in the Wasatch Mountains east of Salt Lake City, Utah (Fig. 2.1). The test was done in late fall during a period of steady streamflow and after riparian leaf-drop. Based on previous experience from similar streams, sodium bromide (NaBr) was injected for 50-hours. The injection time was considered ample for complete exchange of tracer-laden water through the stream and hyporheic transient storage volumes [STS and HTS; *Briggs, et al.*, 2009]. In conjunction with injection, area-velocity stream discharge measurements (Q_{vel}, liters per minute) were made at 13 locations along the reach.

Results showed significant tracer dilution but no net gain in streamflow. Biased by the expectation that exchange times would be less than 50-hours, the findings were initially interpreted as stream-gain from an underlying aquifer (which dilutes tracer) offset by an equal amount of stream-loss to the aquifer (which resulted in no net gain). A more comprehensive examination of the data substantiated that water exchange was balanced but steady-state conditions with respect to stream tracer concentrations (C_{str}, milligrams per liter) were not obtained. Although stream-gain does dilute tracer, it does not create transient C_{str} conditions. Instead the transient conditions are attributed to exchange processes with HTS that exceed 50-hours.

It has been known for some time that transient storage has significant affects on overall stream and near-stream biogeochemistry [*Finley*, 1995]. However, the volume and transit-times quantified at Red Butte Creek exceeds what is normally encountered in mountain catchments. The scale of transient storage at Red Butte likely has broader implications, in terms of late summer water availability to riparian areas, stream/aquifer interactions in downstream reaches, and streamflow amounts/timing during spring snowmelt and precipitation runoff events. The existence of significant transient storage

must be accounted for during any analysis of the mean transit time of water in a drainage basin.

2.3 Site Description

The Red Butte Creek watershed has an area of 18.8 square kilometers (Fig. 2.1) with an altitude range of 1,646 to 2,524 m [*Mast and Clow*, 2000, p. 85]. The watershed is part of the U.S. Geological Survey (USGS) National Benchmark Hydrologic Network. Streamflow has been recorded since 1964 at gaging station 101072200 (Red Butte Creek at Fort Douglas near Salt Lake City). Average 1964-2006 streamflow is 7,360 L/min; baseflow is estimated at 3,740 L/min. A relatively narrow canyon bottom, and steep heavily vegetated hillsides characterize the drainage basin. Unconsolidated stream-channel deposits exist along the canyon bottom. Lower elevation hillside vegetation consists mainly of grass-forb communities, Gambel oak, and bigtooth maple [*Ehleringer and others*, 1992]. Fir and aspen trees are found at the upper elevations of the drainage basin. The predominate soil type is mollisol; these soils are well drained and range in depth from 50 to 150 centimeter [*Woodward*, 1974]. Consolidated rocks underlying the soils consist of limestone, shale, siltstone, sandstone, and quartzite [*Mast and Clow*, 2000, p. 87]. The consolidated rock forms the northern limb of a syncline; the axis of the syncline is approximately parallel to Red Butte Creek [*Van Horn and Crittenden*, 1987]. The creek flows across 4 small fault zones. Most precipitation in the drainage occurs as snowfall during the months of March and April; the driest month is July [*Mast and Clow*, 2000, p. 85].

2.4 Stream-Tracer Test

During October 2003, NaBr was continuously injected into Red Butte Creek for a period of 50 hours. The bromide mass-load of injection ($M_{load\text{-}inj}$, milligrams per minute) was 4,663 mg/min with a variation of +/- 2 %. Water samples were collected over time at 4 sites located 276, 1,902, 3,564 and 4,900 m downstream of the injection location. Single samples were collected from the stream at 29 additional locations. Samples were filtered (less than 0.45 micrometer) and analyzed for Br by ion chromatography to the nearest 0.05 mg/L. Simultaneous with the stream sampling, Q_{vel} was measured at 13 locations using an Acoustic-Doppler Velocity (ADV) meter. Streamflow was gaged at 1,190 L/min during the tracer experiment, at U.S. Geological Survey streamflow gaging station 101072200, located 4,900 m downstream of the injection site. Along the study reach, Parleys Creek is the only tributary stream and there are no surface-water diversions (Fig. 2.1).

2.5 Methods

Fundamental to interpreting the Red Butte dataset is understanding that streamflow was not changing with respect to time (steady state) and C_{str} was changing with respect to time (transient) during the 50-hour test. When streamflow is in steady state, transient C_{str} conditions that exceed initial breakthrough are caused by retention of tracer mass in HTS. The HTS exchange, transit-time distribution, volume, and the physical attributes that create the observed responses can be characterized by examining Q_{vel} and C_{str} of the stream, mass-load in the stream ($M_{load\text{-}str}$, milligrams per minute), and dilution-gaged discharge (Q_{dil}, liters per minute).

Characterizing HTS on the basis of transient C_{str} data requires partitioning

temporary and permanent tracer-mass loss. Temporary mass-loss is created by retention and dispersion in HTS and STS. Permanent mass-loss is created by stream water down welling into the underlying aquifer. When steady state C_{str} is not obtained during the injection period, the amount of temporary mass-loss can only be estimated. Estimation is done using the pattern and total net loss/gain along the reach. A pattern of upstream loss followed by downstream gain is easily conceptualized as HTS exchange. Stream water down wells into the hyporheic zone, travels downstream in the zone, and up-wells back into the stream. Upstream loss to an underlying aquifer followed by downstream gain from a separate hydraulically isolated source, is difficult to conceptualize. This geometry almost inevitably leads to flowpaths that cross one another: crossing flowpaths is not possible in a flow regime induced by potential-energy differences (i.e., groundwater flow). Exclusive gain or loss, or upstream gain followed by downstream loss is more characteristic of stream/aquifer interaction resulting in permanent mass-loss. In addition to the pattern of loss/gain, the net loss/gain also helps separate HTS exchange from stream/aquifer interaction. A small difference in Q_{vel} between upstream and downstream locations (after accounting for tributaries and diversions) is an indicator of HTS exchange. Even if there is some hyporheic flow underneath Q_{vel} measurement locations, net HTS exchange for reaches that are several times longer than the "average" hyporheic flowpath, will be essentially at or near zero. On the other hand it would be unlikely to expect gain from and loss to underlying aquifers to be balanced. However, for all cases where steady-state C_{str} conditions are not obtained during a stream-tracer test, determining the amounts of temporary and permanent mass-loss is qualitative. Partitioning depends to some degree on a combination of physical observations, geologic

setting, and subjective hydrologic judgment.

2.5.1 Water Exchange

Given the inherent uncertainties associated with C_{str} observations that do not reach steady state, it is possible to make reasonable estimates of HTS exchange. To do this, mass-load in the stream ($M_{load\text{-}str}$, milligrams per minute), and the implications in terms of gross water-loss ($water_{gross\text{-}loss}$, liters per minute) and gross water-gain ($water_{gross\text{-}gain}$, liters per minute) are examined. For stream locations where both Q_{vel} and C_{str} are known, $M_{load\text{-}str}$ is calculated as:

$$M_{load-str} = Q_{vel} * C_{str} \quad (1)$$

Stream reaches where $M_{load\text{-}str}$ decreases indicate areas of $water_{gross\text{-}loss}$. The amount of $water_{gross\text{-}loss}$ is estimated using the maximum C_{str} ($maxC_{str}$) measured along the reach and the change in mass load ($\Delta M_{load\text{-}str} = upstrM_{load\text{-}str} - dnstrM_{load\text{-}str}$) as:

$$water_{gross-loss} = \Delta M_{load-str} \Big/ \max C_{str} \quad (2)$$

$\Delta M_{load\text{-}str}$ is positive along reaches where water and tracer is lost (either temporarily or permanently). Once $water_{gross\text{-}loss}$ is estimated, the net exchange of water is measured by the change in area-velocity discharge ($\Delta Q_{vel} = upstrQ_{vel} - dwnstrQ_{vel}$) and $water_{gross\text{-}gain}$ is estimated as:

$$water_{gross-gain} = -\Delta Q_{vel} + water_{gross-loss} \quad (3)$$

The negative sign is required because ΔQ_{vel} becomes negative when downstream

flow is greater than upstream flow.

Because $M_{load\text{-}str}$, $water_{gross\text{-}loss}$, and $water_{gross\text{-}gain}$ are dependent on C_{str}, when C_{str} is not in steady state, calculated values of mass load and gross loss/gain depend on the elapsed time when C_{str} is measured. In the HTS context, steady state and transient are defined for C_{str} conditions after initial tracer breakthrough (created by STS and open-channel velocity). Independent of transient or steady-state C_{str}, along a losing stream reach the relative change in C_{str} between measurement locations is zero. Even though the relative change is constant, tracer mass is being removed from the stream (Q_{vel} decreases in eqn 1). The tracer mass is permanently lost if outflow is to an underlying aquifer, and temporarily lost if outflow is HTS exchange. Along gaining reaches, successive C_{str} decreases downstream during transient conditions. However, unlike losing reaches, decreases vary over time depending on whether gain is from an aquifer or HTS exchange. When gain is from an aquifer (or tributaries) the decrease in C_{str} with distance is independent of time. When gain is due to HTS, C_{str} will shift from decreasing to increasing as HTS progresses toward complete exchange with tracer-laden water. This difference is due to the fact that tracer mass returns to the stream in the HTS scenario.

2.5.2 Transit Times and Volume

As stated, streamflow and Q_{vel} were in steady state and C_{str} in transient state during the stream-tracer test. Assuming C_{str} is zero prior to injection, the time required for C_{str} to reach the steady-state concentration (C_{ss} in milligrams per liter) describes the longest tracer transit-time through the study reach. The C_{str} time-series at a fixed sampling location along the stream is a reasonable estimate of cumulative transit-time of tracer in the STS and HTS volumes between injection and sample locations. Steady state

occurs when C_{str} reaches a steady or plateau concentration at a fixed location over time. This signifies that STS and HTS volumes have completely exchanged with tracer-laden water. A typical C_{str} time series (Fig. 2.2A) consists of a breakthrough, shoulder, and plateau. Initial breakthrough is controlled primarily by STS. The shoulder shape is set by HTS [*Harvey and Wagner, Fig. 5*, 2000], and the plateau concentration is a function of aquifer and tributary inflow to the stream. The breakthrough slope is steep, indicating little hydrodynamic dispersion; the shoulder indicates greater amounts of dispersion created by porous-media flow into, through, and out of HTS. Figure 2.2B shows a schematic of a C_{str} time series created by exchange and dispersion with large HTS volumes. Large HTS creates a systematic and long-term concentration increase after the initial breakthrough and shoulder phase; this is due to longer transit times with larger amounts of dispersion.

To evaluate HTS transit times, the C_{str} time series in Fig. 2.2B is separated at the point where the slope changes from steep to shallow (Fig. 2.3A). Separation is done with the intent to simplify the interpretation of results and implies isolation between STS and HTS. In reality, storage of water in these zones occurs simultaneously. Time-series separation is possible because HTS transit times are significantly longer than STS transit times. The time-point of separation is interpretative and does not have a formal mathematical definition. Minimum hyporheic transit time ($t_{HTS,min}$) and the maximum transit time ($t_{HTS,max}$) define the shortest and longest flowpaths (Fig. 2.3B). The HTS mean transit time (MTT_{HTS}, time) is defined as the elapse time for ½ of the HTS volume to exchange with tracer-laden water, and is estimated as the time when the ratio of C_{str} to C_{str} at $t_{HTS,max}$ equals 0.50.

Concentration can be equated to transit time for the unique conditions created by continuous injection of tracer. That condition is no tracer in the flow system at start of injection (zero-time) and complete inundation of the flow system at steady-state concentration. The transport time imposed by all system processes and mechanisms between injection and monitoring locations are then represented in the C_{str} time series, and the time-series becomes a de-facto plot of cumulative-flow and transit-time. This method of defining MTT_{HTS} is valid given steady-state exchange and concentration at all locations of inflow to the hyporheic zone. During baseflow periods with no precipitation, steady-state exchange is a realistic assumption. However, instream dispersion and STS invalidate the assumption of steady-state inflow concentrations. This problem is minimized when HTS transit times are significantly longer than STS breakthrough, but in all cases becomes more substantial with distance downstream of the injection location. Despite these limitations, the $0.5C_{str}$ provides a framework for estimating MTT_{HTS}. Using the qualified MTT_{HTS} estimate, the HTS volume (Vol_{HTS}, cubic meters) can be calculated as:

$$Vol_{HTS} = MTT_{HTS} * water_{gross-gain} \quad (4)$$

2.5.3 Physical Attributes

The geometry, hydraulic properties, and transport characteristics required to create water exchange and transit times/volume are quantified with the One-Dimensional Transport with Inflow and Storage (OTIS) model [*Runkel*, 1998] and MODFLOW-GWT [*Harbaugh and others*, 2000; *Konikow and others*, 1996]. The simulations are calibrated by matching observed C_{str} time series. OTIS formulates exchange and retention in terms

of mass transfer; MODFLOW-GWT directly replicates flowpaths, hyporheic hydraulics, and downstream transport in the subsurface.

The calibration parameters in OTIS are stream cross-sectional area (A_{str}, square meters), stream longitudinal dispersion coefficient (D_{str}, square meters per second), storage-zone cross-sectional area (A_s, square meters), and 4) exchange coefficient (α, second^{-1}). Although empirical, parameters are obtained directly from stream response to tracer injection and are related to physical characteristics of the stream system. Transient storage is mathematically described as mass-transfer between two volumes of water. The first volume is the open-channel and the second represents pools, eddies, and the porous subsurface [*Runkel*, 1998]. The second pool volume is the sum of STS and HTS volumes. Solving the mass-transfer equation in terms of the decay constant n (time^{-1}) results in:

$$C_{TS}(t) = C_{str}\left(1 - e^{-nt}\right) \; where \quad n = \alpha \frac{A_{str}}{A_s} \tag{5}$$

where C_{TS} is tracer concentration of water in transient storage and t is time. The reciprocal of the decay-constant multiplied by the natural log of 2 (~0.693) is the time required for $C_{TS} = 0.5C_{str}$. The time is when ½ of the open-channel pool has exchanged with the transient storage pool; in OTIS the water exchange is perpendicular to the direction of streamflow. In this paper all transient-storage water exchange is assumed to have a downstream transport component. With that in mind, the decay-constant reciprocal is considered an indicator of the mean transit time of water flowing downstream through the transient-storage volume (MTT_{TS}, time) and is described as:

$$MTT_{TS} = \frac{\ln(2)}{n} \quad or$$
$$MTT_{TS} = \frac{A_s}{\alpha A_{str}} * \ln(2) \tag{6}$$

Parameter estimation is constrained by maintaining a combination of A_s, α, and A_{str} that complies with MTT_{HTS} determined with eqn 4. Whether or not the observed C_{str} time-series can be simulated while adhering to the constraint is a measure of how plausible MTT_{HTS} (eqn 4) is. If a reasonable match is obtained, then A_s in combination with porosity (η), can be used to estimate the cross-sectional area of the stream-channel deposits (A_h, square meters) [*Harvey and others*, 1996] through which water exchange is occurring:

$$A_h = A_s / \eta \tag{7}$$

In MODFLOW-GWT observed Q_{vel} and C_{str} at the injection location, and the average stream gradient are fixed; no underlying or regional-scale aquifer is included in the model domain. Calibration parameters include geometry of the hyporheic zone, spatial variability and absolute values of horizontal and vertical hydraulic conductivities, porosity, and longitudinal and transverse dispersivities. MODFLOW-GWT explicitly simulates the downstream transport of water exchanging through the hyporheic zone. Therefore a simulated MTT_{HTS} can be determined by tracking the modeled breakthrough of an arbitrary transport species with unit concentration. MTT_{HTS} being defined when $C = 0.5C_o$ occurs.

2.6 Results

Results of the stream-tracer test at Red Butte Creek are unique for two reasons: 1) steady-state conditions with respect to the tracer was not obtained within the expected time frame, and 2) near the end of tracer injection there still remained a large discrepancy between Q_{vel} and Q_{dil} at the downstream end of the study reach. Time-series data collected at 276, 1,902, 3,564, and 4,900 m downstream of the injection location show that C_{str} continued to increase during the entire 50-hour tracer injection period (Fig. 2.4A). The injection $M_{load\text{-}str}$ was held constant for the duration of the test at 4,663 milligrams per min (mg/min). The first arrival of bromide at 4,900 m occurred 19 hours after the start of injection. Q_{vel} measurements showed a net increase in streamflow of 220 L/min between the injection location and 4,900 m: this includes 253 L/min of tributary inflow from Parleys Creek (Fig. 2.4B). For the same reach Q_{dil} increased by 5,063 L/min. Q_{dil} is calculated as:

$$Q_{dil} = (injection\ M_{load-str}) * {}^{1}\!/\!_{C_{str}} \quad (8)$$

Within the subreach between 279 and 988 m Q_{vel} measurements showed a net stream-loss of 415 L/min. This is followed by a net stream-gain of 453 L/min for the sub-reach between 1592 to 1902 m. The gain from 3,564 to 3,793 m is tributary inflow from Parleys Creek. The C_{str} profile, collected during the last 12-hours of injection, shows a systematic dilution of tracer along the entire study reach (Fig. 2.4C).

Stream discharge measured at the USGS gaging station located at 4,900 m varied from 1,100 to 1,270 L/min during the 2 weeks prior to and the week of the stream-tracer test. There are no detectable patterns in streamflow variability and variation is considered

noise in the gaged record. Streamflow is judged constant prior to and during the test at an average value of 1,190 L/min.

2.7 Interpretation

Interpretation of Red Butte Creek HTS was done using the described methods. As a starting point it was assumed that stream/aquifer interaction along the study-reach was minimal during the 50-hour stream-tracer test. This conclusion was reached on the basis of the pattern of gain and loss from the stream, as delineated by Q_{vel}. Accounting for Parleys Creek inflow, the change in Q_{vel} between upstream and downstream ends of the study reach is less than 5% of total discharge. This is within the range of measurement error and interpreted as essentially balanced. Therefore if there is any stream/aquifer interaction the $water_{gross\text{-}gain}$ equals the $water_{gross\text{-}loss}$, which seems unlikely. The pattern of upstream loss followed by downstream gain also supports the concept of minimal stream/aquifer interaction. If upstream loss was not the same water that accounts for downstream gain, the aquifer receiving upstream losses would need to be isolated from the aquifer discharging downstream gains. Although fault zones likely influence exchange along the study reach, it is difficult to conceptualize isolated groundwater flow systems at a scale of 4,900 m. For the purpose of this analysis the definition of hyporheic flow by *Harvey and Wagner* [2003] as losing and returning to the study reach of interest, is utilized.

The idea of minimal stream/aquifer interaction changes the concepts of groundwater recharge and flow in the Red Butte catchment. Originally we assumed groundwater recharge was spatially distributed, as a function of precipitation, across the catchment area. In addition, we assumed groundwater discharge occurred along the entire

reach of the stream (Fig. 2.5A). Now groundwater recharge and active groundwater flow are considered focused in the upper altitude areas of the catchment. Groundwater discharge is limited to higher-altitude springs (Fig.2.5B). Streamflow originates at the springs and changes in streamflow reflect HTS exchange.

2.7.1 Water Exchange

Using the C_{str} profile in combination Q_{vel} measurements, $water_{gross\text{-}loss}$, $water_{gross\text{-}gain}$, and $M_{load\text{-}str}$ were calculated for 11 subreaches (Table 2.1). The sum of $water_{gross\text{-}gain}$ is 1,673 L/min. Because C_{str} values used to determine $water_{gross\text{-}gain}$ was not in steady state, it is uncertain how much of the exchange is due to HTS processes. However, it is certain that transient storage processes are occurring. At Red Butte Creek the absence of any large-scale open-channel retention and the time-scale of transient C_{str} specifically indicates HTS processes. Stream/aquifer and tributary exchange is in steady state and is not the cause of transient C_{str}. HTS exchange is occurring, it is just uncertain as to how much. As mentioned, the pattern of stream loss/gain and ΔQ_{vel} both indicate that exchange is entirely related to HTS. Considering uncertainty in both data and methods of interpretation, a probable HTS exchange and associated uncertainty is 1,650 +/- 200 L/min.

For several of the subreaches $water_{gross\text{-}loss}$ is negative, indicating an increase in tracer mass-load. A portion of inflow to the stream from the HTS volume contained tracer, thus some HTS exchange along the reach was completed during the elapsed time between start of tracer injection and stream sample collection. For these reaches, the amount of $water_{gross\text{-}gain}$ represents exchange that did not occur within the elapsed time. For these reaches the sum of $water_{gross\text{-}loss}$ and $water_{gross\text{-}gain}$ (using absolute value for

$water_{gross\text{-}loss}$) is the total exchange. $Water_{gross\text{-}gain}$ values can never be negative because tracer mass is diluted, never lost due to HTS exchange or aquifer inflow.

Tracer dilution due to tributary inflow from Parleys Fork is automatically canceled out of the exchange determination. Tributary inflow decreases C_{str} (because of dilution) in direct proportion to the increase in Q_{vel}. So there is no change in calculated mass-load (eqn 1). Using eqn 2 with $maxC_{str}$ (which occurs above the Parleys Fork) the effect of tracer dilution is removed from the gross loss/gain calculations (eqns 2 and 3).

2.7.2 Transit Times and Volume

HTS transit times along Red Butte Creek were quantified using the C_{str} time-series collected at 276, 1,902, 3,564, and 4,900 m. The time series were separated using the method shown in Fig. 2.3. The times where slope changes occur are listed in Table 2.2 The STS portion of the curve was subtracted from the total elapse times shown for the observed C_{str} time series. Because steady state was not reached during the 50-hour test, the values of MTT_{HTS} and $t_{HTS,max}$ were determined by extrapolation.

Maintaining the assumption of no groundwater interaction, $M_{load\text{-}str}$ at the 4 sites will eventually equal the injection $M_{load\text{-}str}$ (4,663 mg/min). This is true only because Q_{vel} at the 3 sites above Parleys Creek are all about 1,000 L/min (at the gage Q_{vel} is 1,000 L/min plus Parleys inflow). So there is likely very little HTS exchange that is occurring directly underneath the sites. Not having prior knowledge, this was a fortunate happenstance. To estimate the time when $M_{load\text{-}str}$ at the 4 sites equals injection $M_{load\text{-}str}$, the HTS portions of the curve were exponentially extrapolated until C_{str} resulted in a $M_{load\text{-}str}$ of 4,663 mg/min. The exponential extrapolation implies an exponential transit-time distribution for HTS exchange. Rearranging eqn 8 and using the Q_{vel} at each of the

locations, the required C_{str} to equalize $M_{load\text{-}str}$ are listed in Table 2.2 The exponential time constant was determined separately for each time series by minimizing the sum of squared differences between the observed and simulated C_{str} values; observations only exist for a 47-hour or less time-span (Fig. 2.4A). Once the shape of the exponential curve is established, $t_{HTS,max}$ was manually adjusted until the C_{str} values that result in a mass-load of 4,663 mg/min, were obtained (Table 2.2). The time required for C_{str} to reach 1/2 the required concentration represents a "best" estimate of MTT_{HTS}. Using eqn 4, MTT_{HTS}, and the $water_{gross\text{-}gain}$ the estimated Vol_{HTS} for the study reach is 24,100 m^3.

The transit time and volume determined from data at the 4 stream locations represents the aggregation of HTS effects for successively longer portions of the stream reach. For example, the MTT_{HTS} for the 1st reach (279 m of stream) is estimated at 165-hours. At the 2nd reach (1,902 m of stream) estimated MTT_{HTS} is 220-hours. The 220-hour time is an aggregate of transit times for both the first 279 m of stream and the additional 1,623 m of stream. Estimated MTT_{HTS} should increase (or remain neutral) at each successive downstream location.

If all flow in Red Butte Creek were to infiltrate into and re-emerge from HTS within each subreach, then HTS would be a serial process only. The transit-time distribution of successive subreaches could be added. Since not all flow in the creek exchanges into HTS at any given subreach, the HTS process has both a serial and parallel component. An elemental volume of water that exchanges through successive subreaches has a serial transit time. Simultaneous transport of multiple elemental volumes (e.g., 1 elemental volume is moving through the 1st subreach HTS at the same time another elemental volume is transporting through the 2nd subreach) is a parallel process. The C_{str}

time-series aggregates these effects. A unique separation of the serial and parallel effects is not possible, but estimates can be made with the numerical methods discussed in the next section. Regardless of serial or parallel tracer transport, it is not possible for MTT_{HTS} to decease with downstream distance.

Given the fact that MTT_{HTS} cannot decrease, the estimated change in transit time from 220- to 205-hours between 1,902 and 3,564 m is not correct. The source of error is likely due to extrapolation. A subjective estimate based on relative differences and absolute values of successive MTT_{HTS} is that the probable MTT_{HTS} along the reach from 1,902 to 3,564 m is 10 to 20-hours. The minor increase in MTT_{HTS} along the 4^{th} reach is also considered an indication of HTS transit times on the order of 10 to 20-hours. Despite these slight inconsistencies, MTT_{HTS} for the entire study reach is estimated at 240-hours.

Vol_{HTS} is dependent on both MTT_{HTS} and $water_{gross\text{-}gain}$ (eqn 4), and systematically increases with distance downstream (Table 2.2). From the injection location to 1,902 m larger Vol_{HTS} is indicated because MTT_{HTS} gets longer and $water_{gross\text{-}gain}$ increases downstream. For the stream below 1,902 m, MTT_{HTS} becomes slightly longer and increasing Vol_{HTS} is controlled mainly by the increase in exchange. Basically, exchange appears to occur along the entire study reach, but below 1,902 m exchange times become significantly less than upstream of 1,902 m.

2.7.3 Physical Attributes

To quantify the physical attributes of the hyporheic zone along Red Butte Creek, the computer program OTIS was used to simulate in-stream transport and tracer retention created by the aggregated effects of STS and HTS. The OTIS simulation includes the entire 4,900 m study reach. Tracer exchange and transport through the hyporheic zone

were examined using MODFLOW-GWT. The MODFLOW-GWT simulation was designed to look specifically at hyporheic transport and the domain is sized to match transport lengths of 50 to 100 m. The entire study reach is not simulated, nor is in-stream transport and STS.

2.7.3.1 Stream Transport and Concentration Time-Series

On the basis of mass-load and concentration time-series concentration considerations, hyporheic exchange and MTT_{HTS} are estimated at 1,650 L/min and 240-hours, respectively. These values are assessed by numerically simulating the observed conditions. OTIS was calibrated in a stepwise manner to the measured C_{str} time-series data for locations at 276, 1,902, 3,564, and 4,900 m below the injection location (Fig. 2.6A). The stream was separated into 4 reaches that correspond to the monitoring locations (Table 2.3). Tributary inflow from Parleys Creek is simulated; no additional inflow or outflow was simulated. Each reach was discretized into 5 m sections. A_{str} was adjusted to control timing slope of the breakthrough. D_{str} was used to control early-time plateau concentration. A_s was increased to reduce plateau concentrations and α was increased to reduce the initial concentration of the plateau. Once a reasonable solution was established, the parameters were finalized using UCODE (*Poeter and others,* 2005) to minimize the sum of squared differences between the observed and simulated C_{str} values. The solution was constrained by the extrapolated MTT_{HTS} determined with eqn 6 and listed in Table 2. OTIS treats transient storage as a single entity, as corresponding to the observed time-series (time-series separation is interpretive, not observed). As such, A_s includes both STS and HTS. For Red Butte Creek, where open-channel retention is a minor element of the observed transient conditions, MTT_{TS} derived in eqn 6 is considered

equivalent to MTT_{HTS}. The best fit to observed C_{str} was achieved using the parameter values listed in Table 2.3. Plots of simulated and observed C_{str} values are shown on Fig. 2.6A.

In general, the OTIS simulation is a reasonable representation of observed conditions. For all but the 2nd reach, the simulated plateau slope is somewhat greater than observed. Steeper slope means simulated tracer retention in transient storage is shorter than observed. A better fit to observations is possible but only if the MTT constraint is exceeded; the current solution is at or near the upper limit (Table 2.3). Considering that OTIS aggregates the serial and parallel aspects of tracer transport, total MTT_{TS} are the simulated values, and represent the aggregated time for the upstream reaches. Individual reach MTT_{TS} are calculated as the difference between successive reaches. Simulated MTT_{TS} for the study reach is 274-hours, which is about 15% longer than the 240-hour MTT_{HTS} based on time-series separation and extrapolation. Using eqn 7 with the average A_s value (12.6 m^2) and a porosity of 0.20, A_h is estimated at 63 m^2.

Using the calibrated OTIS simulation, the injection period was lengthened until tracer concentration reached a steady-state value at 4,900 m (Fig. 2.6B). The projected time to reach steady state is approximately 2,100 hours (87 days) and illustrates both the extended time frame to achieve complete exchange, and that ½ of the transient storage volume is exchanged within the first 10% of the longest transit time.

2.7.3.2 Hyporheic Transport and Exchange

To estimate hyporheic zone hydraulic and transport parameters, the observed tracer response along the 1st and 2nd reach of the stream (0 to 1,902 m) was simulated using MODFLOW-GWT. Parameters were estimated by minimizing the difference

between simulated concentrations and the observed C_{str} time-series at 276 and 1,902 m. Also, the difference between estimated and simulated exchange is minimized (Table 2.2). Matching the observed C_{str} implicitly means that the MTT_{HTS} values listed in Table 2.3 are reasonably simulated. When exchange is also reproduced, then Vol_{HTS} is matched (eqn 4). Assuming that η ranges between 0.10 and 0.30, the relationship Vol_{HTS}/η was used to ascribe an initial model domain that is 22 m wide, 12 m thick, and 500 m long. The domain is essentially a long rectangular box; grid cells are 2 m on a side (8 m^3). The active area of the model is adjusted to create estimated exchange, η is adjusted to control transport velocities. To ease display and manipulation of parameters, the model is sized to approximate the physical dimensions of hyporheic transport, not the actual stream length.

The stream is simulated using the Streamflow Routing Package (SFR; *Niswonger and Prudic,* 2003). SFR simulates for mixing with inflowing waters of varied concentration; it does not simulate stream transport (as does OTIS). Two stream segments are used; the initial concentration for the 1st segment is specified at the injection amount of 4.81 mg/L. Input to the 2nd segment is the simulated C_{str} time-series output from the 1st segment; this reproduces the aggregated effects of serial and parallel transport created by successive HTS exchange with the stream. The flow field is simulated at steady state; tracer transport is simulated for 314.5-hours (13 days), using 2-transport stress periods. Two transport stresses were used to account for in-stream transport times, which are not explicitly simulated.

The model domain is split by a vertical swath of inactive cells creating 2 sub-domains with lengths of 100 and 398 m (Fig. 2.7A). The subdomains represent hyporheic

circulation between the injection location and 276 m, and 276 to 1,902 m, respectively. The inactive cells force all hyporheic exchange to return to the stream boundary at the location of the vertical swath. Initially horizontal and vertical hydraulic conductivities (K_h and K_v, meters per day), and streambed conductivity (K_{str}, meters per day) were adjusted to try and match the 463 and 586 L/min of estimated hyporheic water exchange (Table 2.1). The next calibration step was adjusting η, and dispersivity to match the observed C_{str} time series for 276 and 1,902 m. Since flow is in steady state, simulated C_{str} at 100 and 500 m is a function of the initial stream-boundary concentration (4.81 mg/L), and the simulated amount of tracer mass re-emerging from HTS. As a consequence, the change in C_{str} at 100 and 500 m is controlled by the amount of exchange with HTS, and the transit time of water through the HTS volume.

Modeling objectives are to simulate exchange amounts and flowpath lengths that result in a reasonable match to observed C_{str} time-series. Individual parameter values were not constrained nor varied on a cell-by-cell basis. The observed C_{str} time series at 276 m can be reproduced with flowpath lengths of 100 m (Figs. 2.7 and 2.8A). The observed C_{str} time series at 1,902 could not be reproduced with 400 m flowpaths; simulated transit times are too long. Inactivating model cells to create a series of 50 m long HTS circulation cells, (Fig. 2.7B) a replication of observations was realized (Fig. 2.8B). For both reaches the simulated water exchanges are about 60% of the estimated values (Tables 2.1 and 2.4). The simulated MTT_{HTS} values are about 75% of the extrapolated values (Tables 2.2 and 2.4). Additional calibration could likely decrease the mis-fit between simulated and estimated/extrapolated values. However, the visual fit to the observed time-series is good, particularly at 276 m (Fig. 2.8A).

2.8 Discussion and Conclusions

After 50-hours of tracer injection Red Butte Creek C_{str} did not reach steady-state conditions along the 4,900 m study reach. Given that streamflow and injection were in steady state, the transient C_{str} conditions are created by HTS with transit times that exceed 50-hours. The transient conditions require modification to the standard methods used to define the hyporheic zone interaction. This paper describes those modifications as they relate to 1) gross-water exchange, 2) transit times and volume, and 3) hydraulic characteristics of the HTS.

For stream locations where both Q_{vel} and C_{str} were quantified, $M_{load\text{-}str}$ was calculated and used to quantify $water_{gross\text{-}loss}$ from the stream and $water_{gross\text{-}gain}$ to the stream. Results show water exchange into and out of HTS is 1.5-times greater than stream discharge (1,650 versus 1,190 L/min). The C_{str} time series, which were collected at 4 stream locations, were separated into STS and HTS components, to qualify transit times. The HTS component was exponentially extrapolated until C_{str} resulted in a $M_{load\text{-}str}$ equal to the injection $M_{load\text{-}str}$ (4,663 mg/min). The time required for C_{str} to reach 1/2 the concentration required for mass balance was considered a "best" estimate of MTT_{HTS}. In addition to mass balance and time-series separation, numerical simulations of stream and hyporheic transport were simulated using OTIS and MODFLOW-GWT. Using MTT_{HTS} derived from time-series separation, OTIS can successfully reproduce observed C_{str} time-series, which adds credibility to estimated/extrapolated values. MODFLOW-GWT also reproduces the observed time series.

There are inconsistencies between estimates of exchange, transit times, and volume, using the various methods of interpretation. Exchange determined from mass

balance is about 1.5 times more than estimated by MODFLOW-GWT. MTT_{HTS} and Vol_{HTS} extrapolated from time-series separation and mass balance are also about 1.5 times more than indicated by MODFLOW-GWT simulations. Also, MTT_{HTS} from extrapolation does not get progressively longer with downstream distances. MODFLOW-GWT simulation also shows that observed conditions require extremely permeable stream-channel deposits, with hydraulic conductivities of up to 200 m/d.

When considering that the tracer-test conducted in Red Butte Creek was not designed to quantify large HTS, the methods introduced in this paper quantify a reasonable framework of hyporheic-zone characteristics. The amount of HTS exchange is on the order of 1,200 to 1,600 L/min; MTT_{HTS} is at least 200-hours; Vol_{HTS} is in the range of 20,000 m^3; and HTS flowpaths occur on the scale of 10 to 100 m. It also appears that most of the HTS is located in the upper 2,000 m of the study reach. To speculate, the large HTS estimated for Red Butte Creek might be related to observed tufa structures coupled with the landslide/mass wasting features that exist in the canyon. This could create spatially limited but high conductivity zones underneath the creek that could create large HTS and water exchange at a spatial scale of 50 to 100 m.

2.9 Acknowledgements

The following people are noted for their discussion of results, manuscript reviews, field work, data collection, and laboratory analysis: Ken Bencala, Suzanne Bethers, Andrew Burr, Katie Walton-Day, Terry Kenny, Judy Steiger, Don Semon, and two anonymous reviewers. This work was funded largely by National Science Foundation, Award # 0309212. The U.S. Geological Survey Toxics Program supported the sodium-bromide tracer injection and laboratory analysis.

2.10 References

Briggs, M. A., M. N. Gooseff, C. D. Arp, and M. A. Baker (2009), A method for estimating surface transient storage parameters for streams with concurrent hyporheic storage, *Water Resour. Res., 45*.

Ehleringer, J. R., L. A. Arnow, T. Arnow, I. B. McNulty, and N. C. Negus, (1992), Red Butte Canyon Research Natural Area-History, flora, geology, climate, and ecology, *Great Basin Naturalist, 52*, 95-121.

Finley, S., (1995), Importance of surface-subsurface-exchange in stream ecosystems: The hyporheic zone, *Limnology and Oceanography, 40*, 159-164.

Harbaugh, A. W., (2005), MODFLOW-2005, The U.S. Geological Survey modular ground-water model—the ground-water flow process, *U.S. Geol. Surv. Tech. and Meth. 6-A16*.

Harvey, J. W., and B. J. Wagner, (2000), Quantifying hydrologic interactions between streams and their subsurface hyporheic zones, in *Streams and Ground Waters*, edited by J. A. Jones and P. J. Mulholland, pp. 3-43, Acad. Press, San Diego, CA.

Konikow, L. F., D. J. Goode, and G. Z. Hornberger, (1996), A three-dimensional method-of characteristics solute-transport model (MOC3D), *U.S. Geol. Surv. Water Resour. Invest. Rep. 96-4267*, 87 p.

Mast, M. A. and D. W. Clow, (2000), Environmental characteristics and water quality of hydrologic benchmark network stations in the western United States, 1963-95, *U.S. Geol Surv. Circ. 1173-D*, 114 p.

Niswonger, R. G. and D. E. Prudic, (2003), Documentation of the Streamflow-routing (SFR2) Package to include unsaturated flow beneath streams-A modification to SFR1, *U.S. Geol. Surv. Tech. and Meth. 6-A13*, 50 p.

Poeter, E. E., M. C. Hill, E. R. Banta, S. W. Mehl, and S. Christensen, (2005), UCODE-2005 and six other computer codes for universal sensitivity analysis, calibration, and uncertainty evaluation; constructed using the JUPITER API, *U.S. Geol. Surv. Tech. and Meth. 6-A11*, 283 p.

Runkel, R. L., (1998), One-dimensional transport with inflow and storage (OTIS): A solute transport model for streams and rivers, *U.S. Geol. Surv. Water Resour. Invest. Rep. 98-4018*, 70 p.

Van Horn, Richard, and M. D. Crittenden Jr., (1987), Map showing surficial units and bedrock geology of the Fort Douglas quadrangle and parts of the Mountain Dell and Salt Lake North quadrangles, Davis, Salt Lake, and Morgan Counties, *Utah, U.S. Geol. Surv. Misc. Invest. Series Map I-1762*, scale 1:24,000.

Woodward, Lowell, (1974), Soil survey of Salt Lake area, Utah, *U.S. Depart. of Agri. Soil Conser. Service*, 132 p.

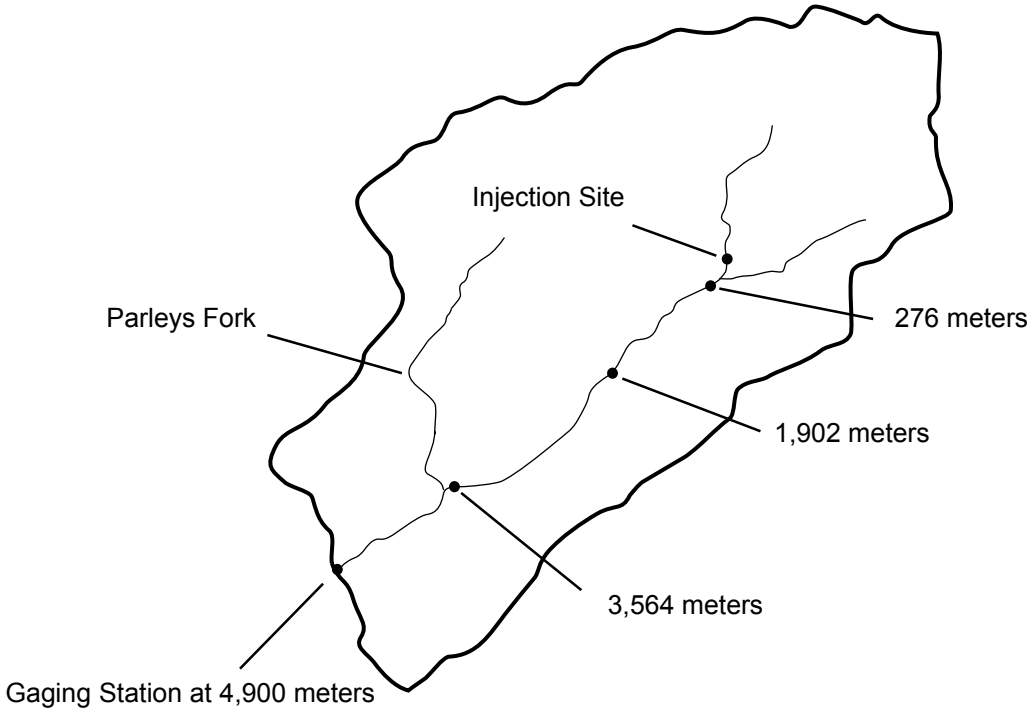

Figure 2.1 Location map of the study area, Red Butte Creek in the Wasatch Mountains, Salt Lake County, Utah.

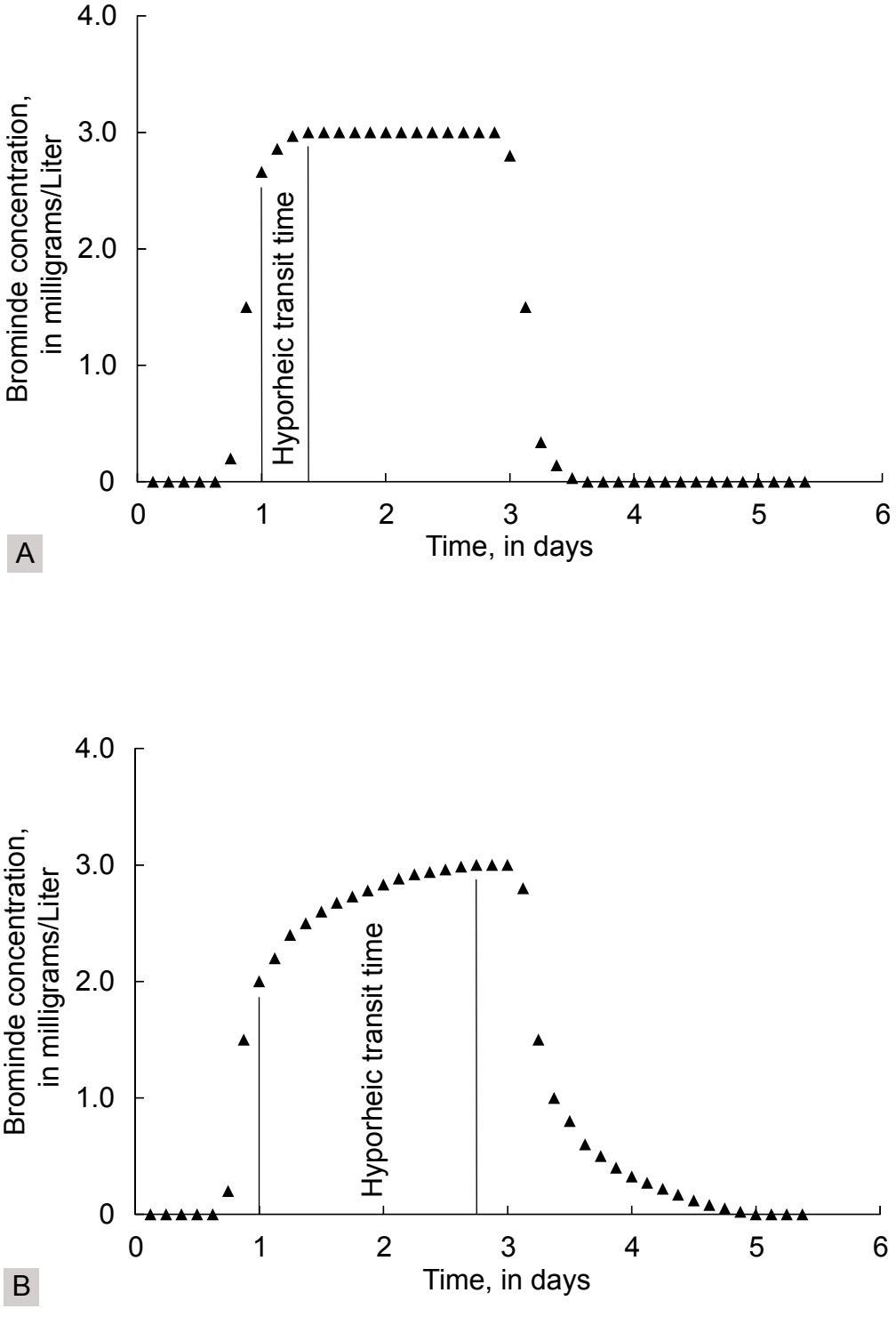

Figure 2.2 Hypothetical stream concentration time series for A) a stream with typical hyporheic storage, and B) a stream with large hyporheic transient storage.

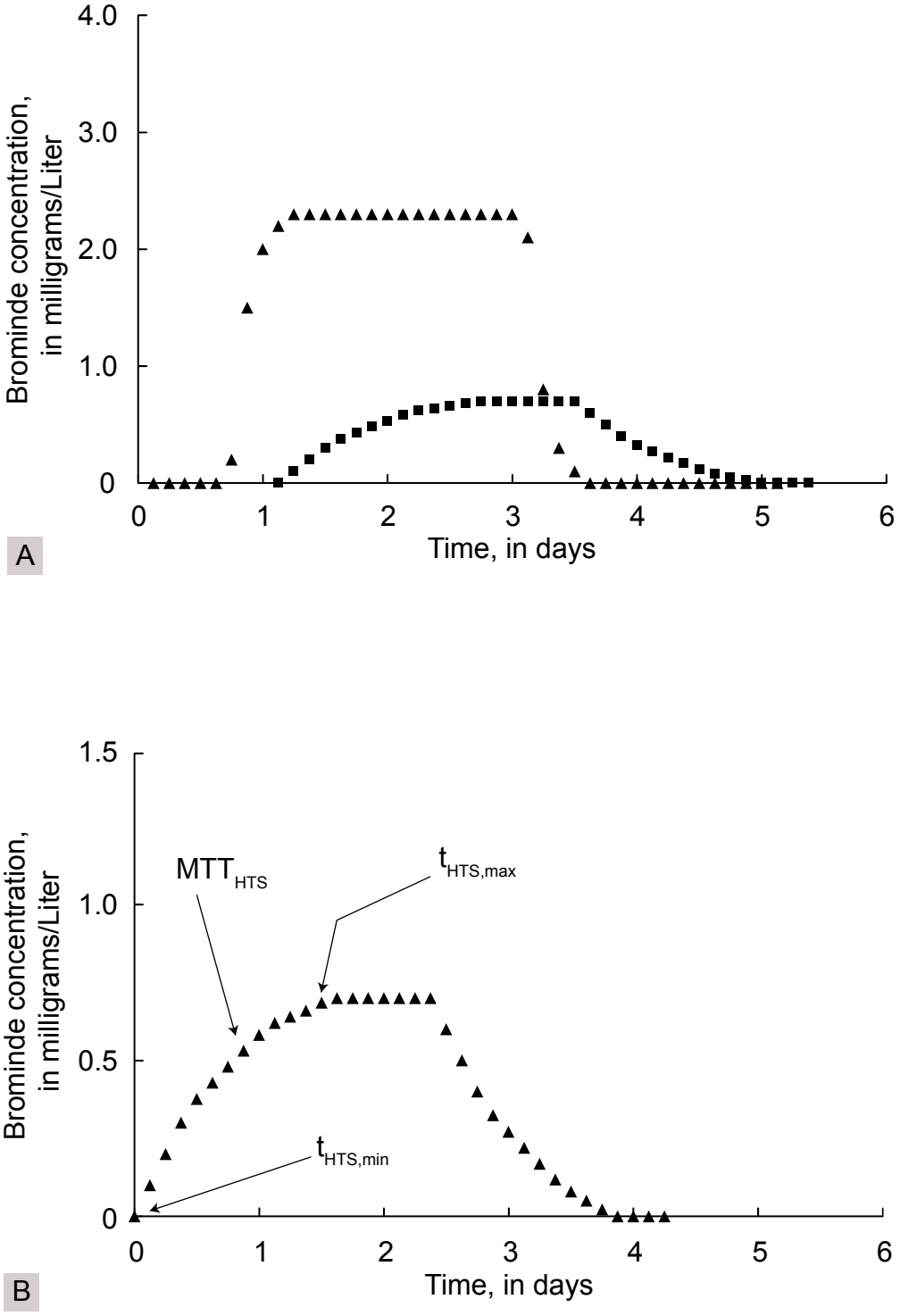

Figure 2.3 Hypothetical stream concentration time series A) separation into stream-transient-storage and hyporheic-transient-storage components, and B) hyporheic transient storage time series with minimum, maximum, and mean transit times.

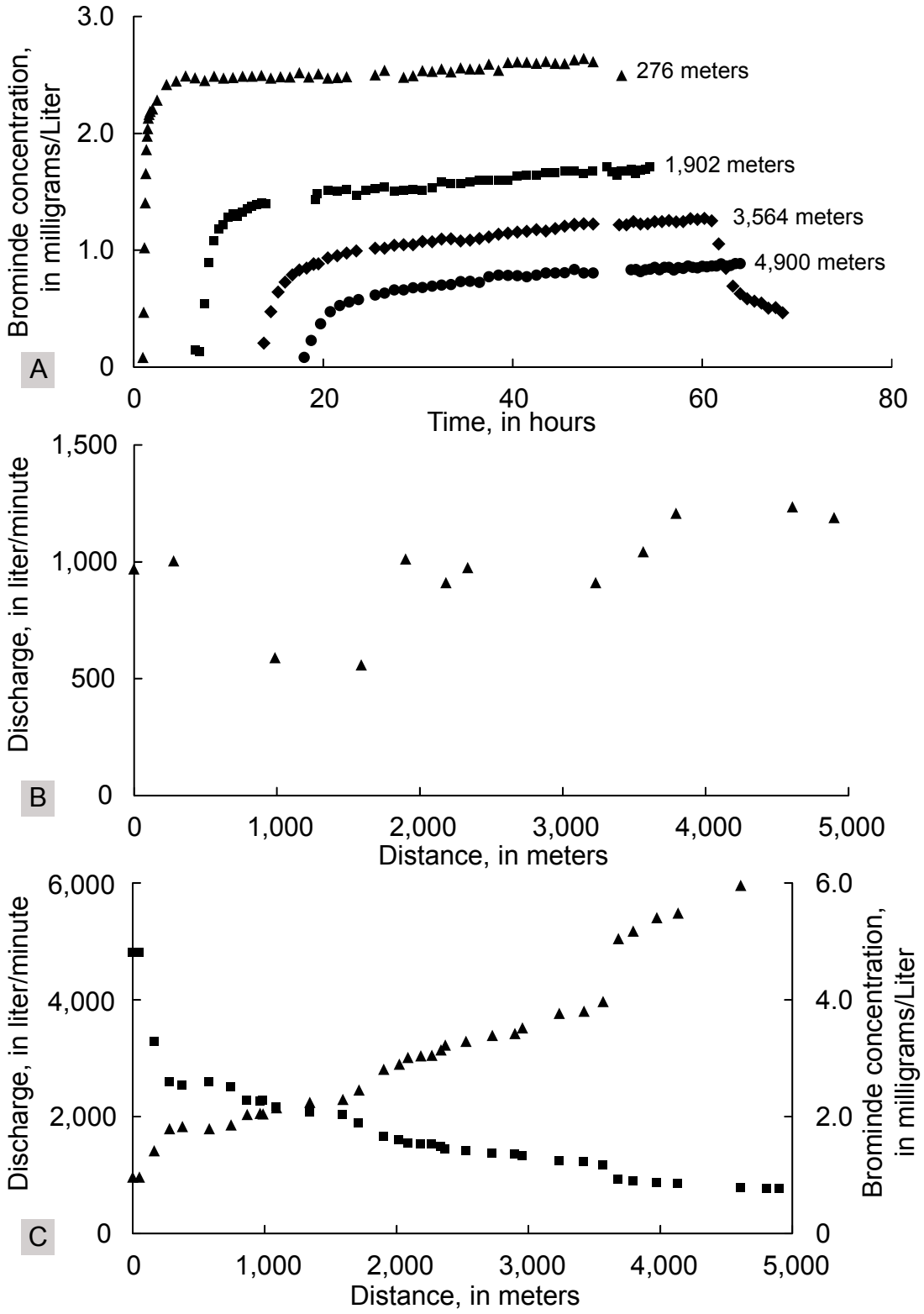

Figure 2.4 Graphs showing A) stream-water bromide concentration time-series at 4 fixed locations, B) area-velocity discharge at 12 locations, and C) dilution discharge and stream-water concentration profiles, Red Butte Creek in the Wasatch Mountains, Salt Lake County, Utah.

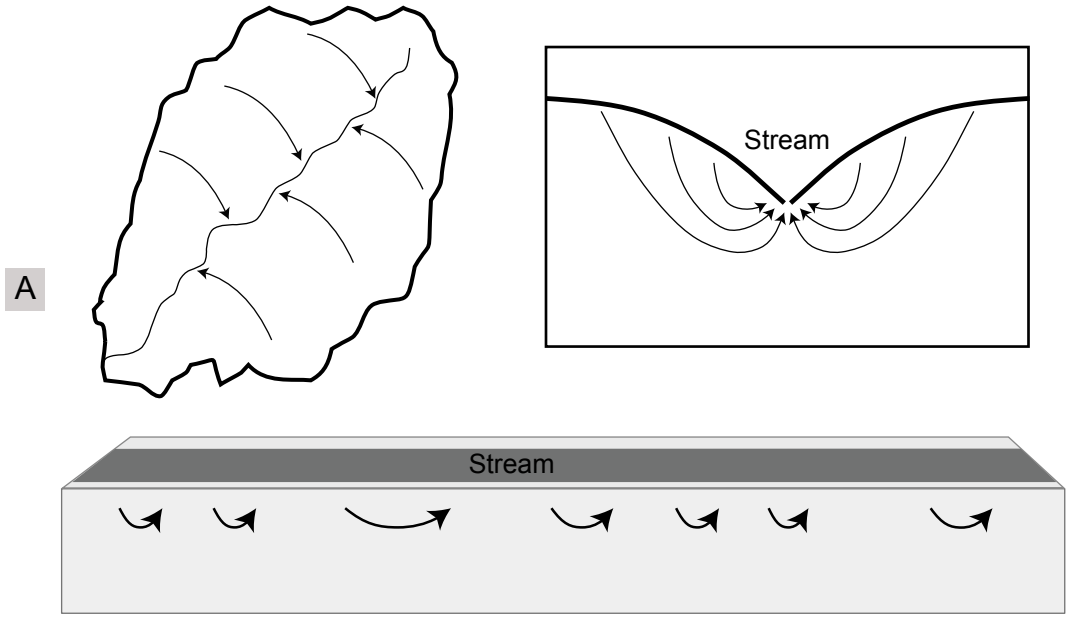

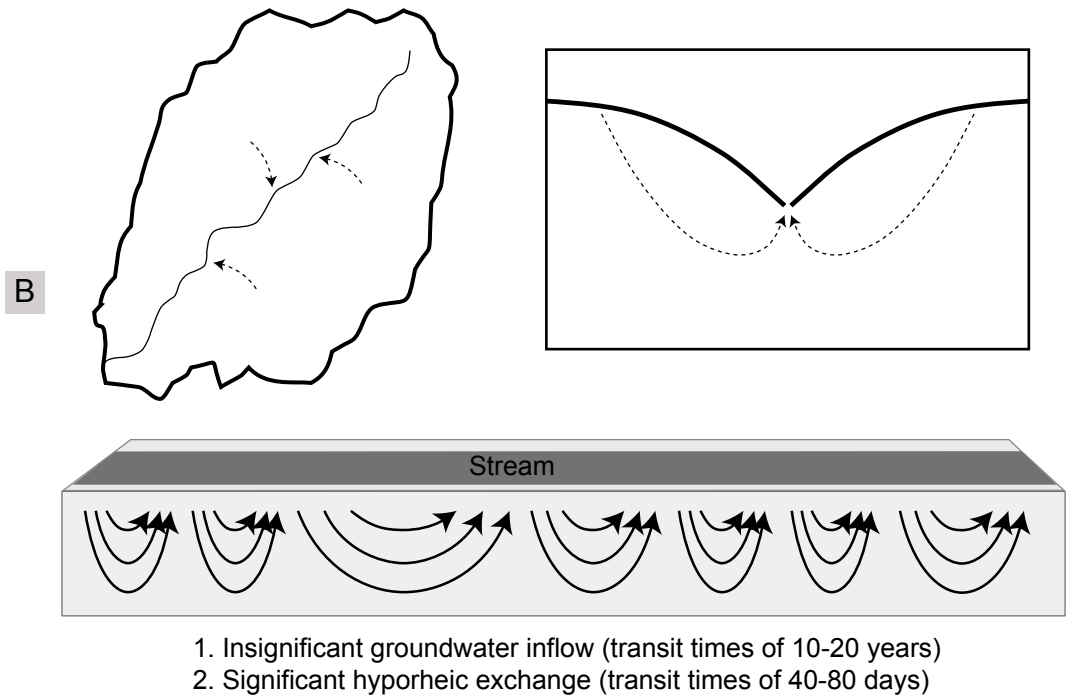

Figure 2.5 Schematic diagrams showing the A) original, and B) revised conceptual models of groundwater flow, Red Butte Creek in the Wasatch Mountains, Salt Lake County, Utah.

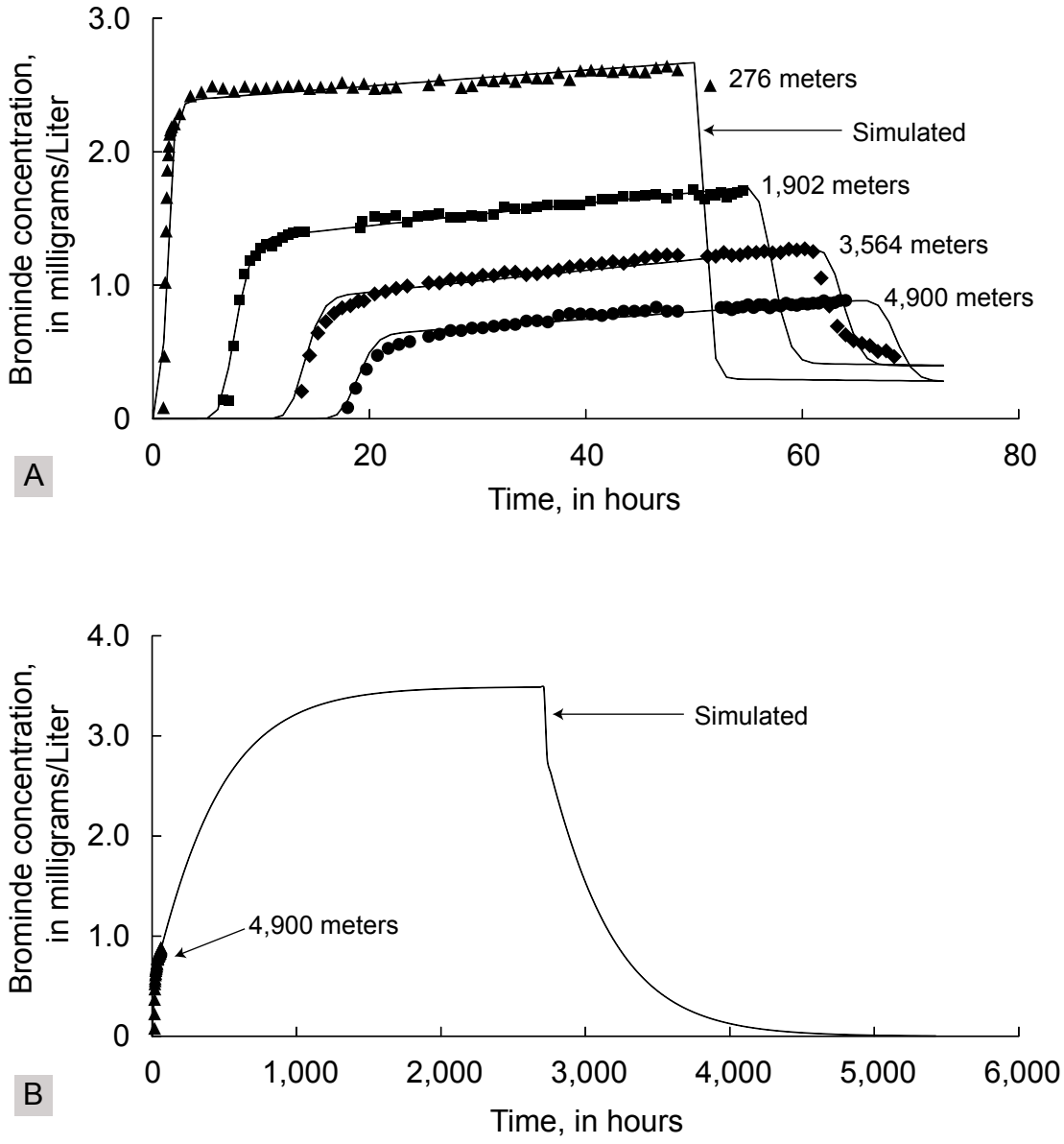

Figure 2.6 Plots of A) OTIS results and observed time-series concentrations at 4 monitoring location, and B) OTIS simulation to steady-state concentration at 4,900 meters, Red Butte Creek in the Wasatch Mountains, Salt Lake County, Utah.

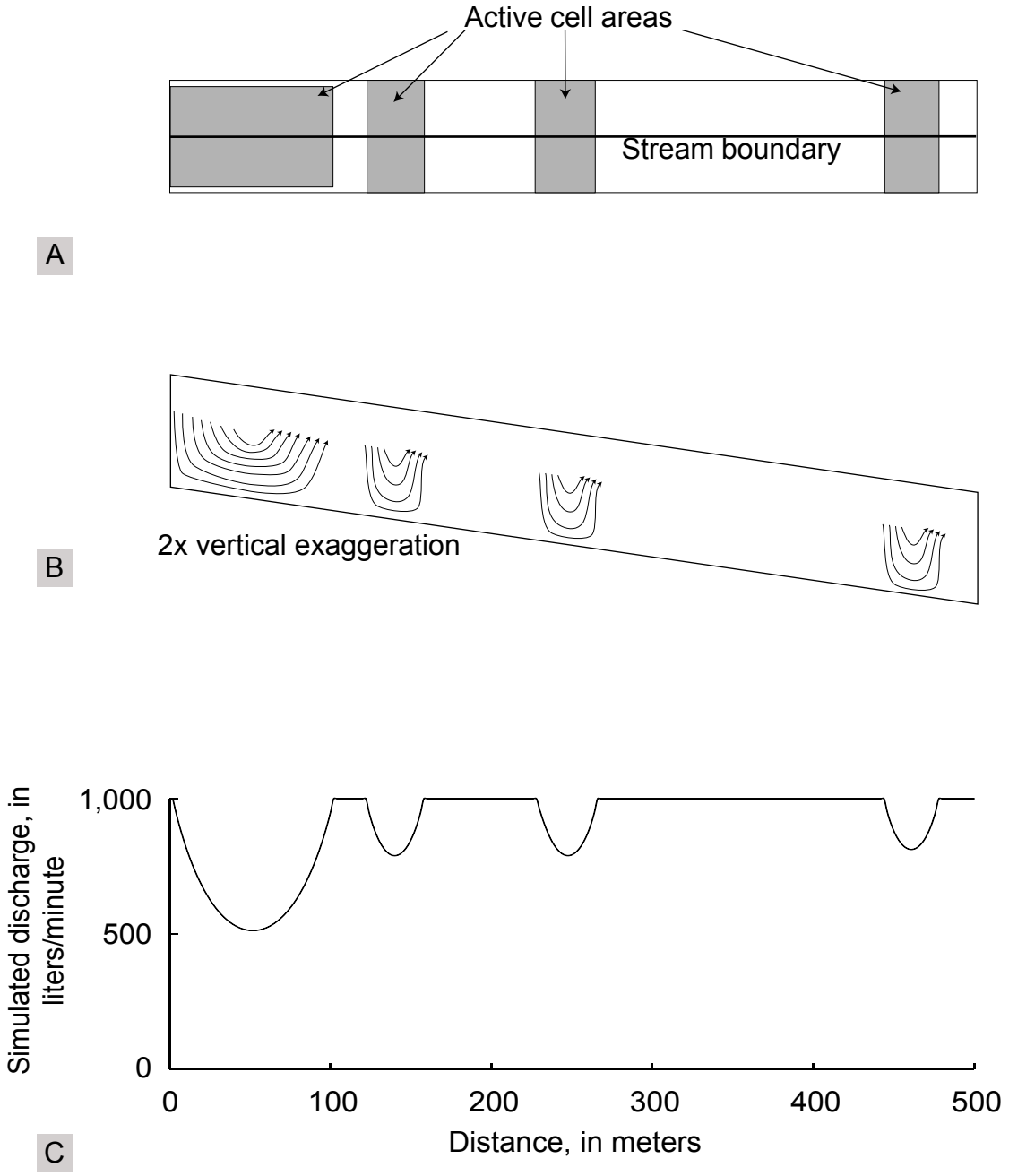

Figure 2.7 MODFLOW-GWT A) model domain in plan view, B) simulated flowpaths in cross-sectional view, and C) simulated streamflow, Red Butte Creek in the Wasatch Mountains, Salt Lake County, Utah.

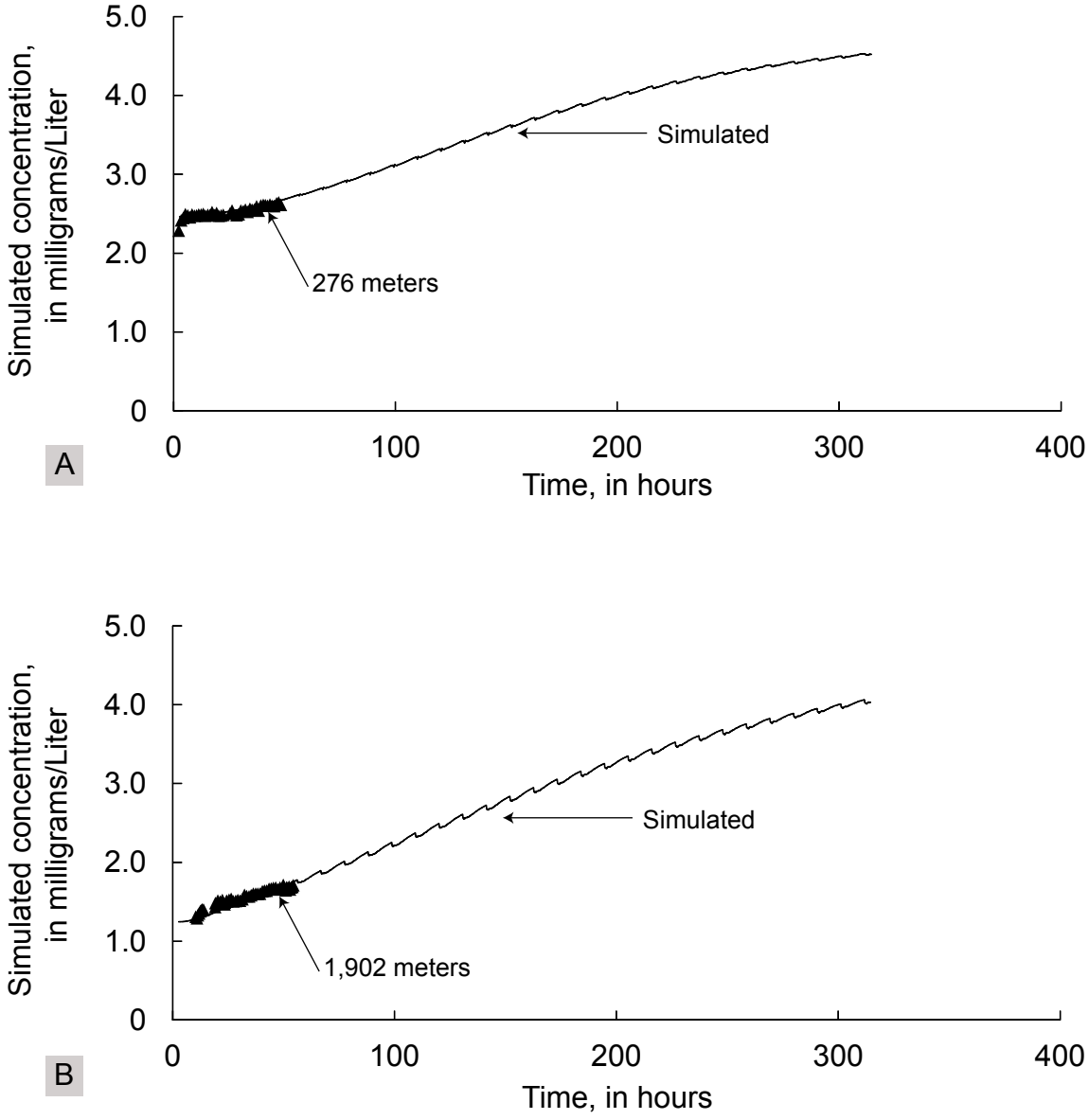

Figure 2.8 MODFLOW-GWT simulated concentration time series and observed stream concentration time series at A) 276 m and B) 1,902 m, Red Butte Creek in the Wasatch Mountains, Salt Lake County, Utah.

Table 2.1 Stream concentration, area-velocity discharge measurements, mass-load in the stream,and gross water loss and gain, Red Butte Creek in the Wasatch Mountains, Salt Lake County, Utah.
(delta Mass-load-stream; positive represents reduction in mass-load-stream, negative represents gain in mass-load-stream

Stream ID	Distance	Bromide concentration in stream (mg/L)	Q-velocity (liters/min)	Mass-load-stream (mg/min)	delta Mass-load-stream (mg/min)	Water gross-loss (L/min)	Water gross-gain (L/min)	Total hyporheic transient storage exchange (L/min)	Reach hyporheic transient storage exchange (L/min)
0	0	4.81	970	4,666					
163	163	3.29							
279-T1	279	2.59	1,004	2,603	2,063	429	463	463	463
376	376	2.54							
580	580	2.59							
746	746	2.50							
868	868	2.29							
965	965	2.27							
988	988	2.27	589	1339	1264	487	73	536	
1,090	1,090	2.16							
1,343	1,343	2.08							
1,592	1,592	2.03	559	1134	205	90	60	596	
1,715	1,715	1.90							
1,902-T2	1,902	1.66	1,012	1,677	-543	-267	186	1,050	
2,021	2,021	1.61							586
2,086	2,086	1.55							
2,183	2,183	1.53	911	1,394	283	171	69	1,119	
2,266	2,266	1.53							
2,336	2,336	1.48	975	1,446	-51	-34	31	1,184	
2,369	2,369	1.44							
2,525	2,525	1.42							
2,725	2,725	1.37							
2,896	2,896	1.36	1,364	note: this area-velocity discharge measurement was not used					
2,953	2,953	1.32							
3,232	3,232	1.24	911	1,125	321	216	152	1,336	
3,419	3,419	1.22							
3,564-T3	3,564	1.17	1,043	1,224	-99	-80	53	1,468	
3,605	3,605	0.00	253	note: tributary inflow from Parleys Creek					417
4,481	3,681	0.92							
4,593	3,793	0.90	1,208	1,087	137	117	29	1,497	
4,772	3,972	0.86							
4,933	4,133	0.85							
5,408	4,608	0.78	1,235	966	121	134	162	1,659	
5,604	4,804	0.77							
5,700-T4	4,900	0.77	1,189	919	47	60	14	1,673	
									204

Table 2.2 Hyporheic transient storage transit times and volume estimates, Red Butte Creek in the Wasatch Mountains, Salt Lake County, Utah.

Site ID	Distance (meters)	Time of separation (hr since start of injection)	Initial stream concentration (mg/L)	Final stream concentration (mg/L)	Final stream transient storage component (mg/L)	Final hyporheic transient storage component (mg/L)	1/2 hyporheic transient storage component concentration (mg/L)	Time constant (1/hr)	Mean hyporheic transient storage transit time (hours)	Longest hyporheic transient storage transit time (hours)	Hyporheic transient storage exchange (L/min)	Hyporheic transient storage volume using equation 5 (m3)
T-1	279	2.5	0	4.65	2.28	2.37	1.18	0.0225	165	1,760	463	4,600
T-2	1,902	10.5	0	4.61	1.31	3.30	1.65	0.0029	220	2,080	1,050	13,900
T-3	3,664	17.5	0	4.47	0.83	3.64	1.82	0.0034	205	1,820	1,468	18,100
T-4	4,900	21.75	0	3.92	0.53	3.39	1.70	0.0029	240	2,070	1,673	24,100

Table 2.3 OTIS exchange parameters and corresponding hyporheic transient storage mean transit times, Red Butte Creek in the Wasatch Mountains, Salt Lake County, Utah.

Reach Number	Starting distance (m)	Ending distance (m)	Length (m)	A_{str} (m^2)	D_{str} (m^2/sec)	A_s (m^2)	a (1/sec)	Total MTT_{TS} (hours)	Reach MTT_{TS} (hours)
1	0	276	276	0.3	2.00	45.0	0.000170	170	170
2	276	1,899	1,623	0.23	1.00	2.2	0.000027	238	68
3	1,899	3,561	1,662	0.23	1.50	2.0	0.000016	248	10
4	3,561	3,678	117	0.23	0.25	No hyporheic exchange simulated for reach 4			
5	3,678	4,897	1,219	0.23	0.25	1.3	0.000042	274	26

Table 2.4 MODFLOW-GWT with Streamflow Routing Package hyporheic zone hydraulic parameters, mean transit times, and volume, Red Butte Creek in the Wasatch Mountains, Salt Lake County, Utah.

Reach Number	Starting distance (m)	Ending distance (m)	Length (m)	Horizontal hydraulic conductivity (m/day)	Vertical hydraulic conductivity (m/day)	Streambed conductivity (m/day)	Porosity (unitless)	Longitudinal dispersivity (m^2/day)	Vertical and horizontal transverse dispersivity (m^2/day)	Diffusion coefficient (1/day)	Total MTT_{HTS} (hours)	Reach MTT_{HTS} (hours)	Hyporheic transient storage exchange (L/min)	Hyporheic transient storage volume (m3)
1	0	100	100	200	200	125	0.25	5.0	0.0	0.0	126	126	295	5,000
2	100	500	400	125	125	100	0.15	5.0	0.0	0.0	167	40	368	3,308

CHAPTER 3

DETERMINATION OF FLOW-WEIGHTED AVERAGE GROUNDWATER CHLOROFLOUROCARBON-12 CONCENTRATIONS FROM STREAM WATER SAMPLES: A CASE STUDY AT THE SIXMILE SYSTEM, TOOELE VALLEY, UTAH

3.1 Abstract

The Sixmile System is a regional groundwater discharge location within the Tooele Valley groundwater basin, Utah. The concentration of a dissolved constituent in the discharging water represents a flow-weighted average of all groundwater flowpaths that are converging at the location. Because chloroflourocarbon-12 is a volatile constituent, determining its concentration consists of accurately measuring specific-discharge and the gas-exchange characteristics, then numerically simulating gas transport. The Sixmile System consists of Sixmile Spring and 593 m of the 1st order stream that originates at the spring. Combined discharge of the system at 593 m is 82.9 L/sec. Bromide dilution quantified specific discharge of groundwater to the stream below the spring ranging from 1.2 x 10^{-4} to 1.1 x 10^{-5} m/sec. On the basis of a gas-injection tracer test, the average gas-exchange velocity of chloroflourocarbon-12 in the stream is estimated at 0.48 m/d. Observed chloroflourocarbon-12 concentrations (C_{CFC-12}) in stream water varied from 0.91 to 1.37 pmoles/kg of water, which is below the air-equilibration

value of 2.25 pmoles/kg of water. Using the groundwater inflow, gas-exchange velocity, and observed stream-water concentrations, the groundwater inflow C_{CFC-12} was estimated by simulating gas transport. The best fit to observed conditions results from a simulated groundwater-inflow C_{CFC-12} of 1.16 pmoles/kg of water; the 95% confidence interval is 0.94 to 1.37 pmoles/kg of water. This is considered the flow-weighted average C_{CFC-12} of groundwater discharging at the Sixmile System. To assess the validity of the simulated concentration, 10 piezometers were installed along the study reach and sampled for chloroflourocarbon-12. The piezometer samples ranged in C_{CFC-12} from 0.31 to 1.38 pmoles/kg of water. Those concentrations, when weighted by the groundwater inflow in accordance to groundwater inflow amounts, resulted in a flow-weighted average C_{CFC-12} of 1.08 pmoles/kg of water. The level of agreement between the simulated and directly measured groundwater concentrations suggest that for a stream setting where the ratio of gas-exchange velocity to specific discharge of groundwater is less than 0.13, a good estimate of the flow-weighted average groundwater C_{CFC-12} can be derived from stream samples. Furthermore, the fact that only one stream-water C_{CFC-12} falls outside the 95% confidence interval of the simulated groundwater inflow implies that for a ratio of 0.13, gas-exchange has only a minor influence on the stream-water concentrations.

3.2 Introduction

Locations where groundwater flowpaths converge and discharge to the surface (e.g., springs and gaining streams) provide useful and robust observational data. Flow and water-quality attributes represent and respond to forcing processes/mechanisms that have been averaged or smoothed by aquifer heterogeneities. Chloroflourocarbon-12 is a gas dissolved in water that has the potential to quantify an apparent age for groundwater. The

$C_{CFC\text{-}12}$ (pmoles/kg of water) of spring and gaining stream waters is a flow-weighted average that can be equated to the mean transit time (MTT) of the discharging groundwater. Spring discharge identifies the flux of water, the range of transit times describes the spatial distribution of recharge, and MTT quantifies the volume of groundwater storage, within the contributing area [*Cook and Bohlke*, p. 9, 2000). The complicating factor of sampling volatile gases such as chloroflourocarbon-12 from stream water is that concentrations are not conserved. As soon as groundwater discharges and is exposed to the air-water interface, dissolved chloroflourocarbon-12 begins to equilibration with the atmosphere and the groundwater signal begins to degrade.

To correct for atmospheric equilibration, gas-exchange velocities and the rate of groundwater inflow to a stream need to be quantified. Gas-exchange velocities are specific for a given gas and stream morphology and are quantified by injecting the gas at concentrations several orders of magnitude above ambient levels, into the stream and measuring downstream concentration changes. Groundwater inflow can be measured by dilution of a soluble conservative tracer as a function of downstream distance. Using the gas-exchange and groundwater inflow information, the one-dimensional advection-dispersion equation can be numerically solved for the gas concentrations of inflowing groundwater that would create a unique profile of stream water gas concentrations. The experiment described in this paper tests the validity of the gas-exchange correction methodology by comparing corrected gas concentrations to groundwater $C_{CFC\text{-}12}$ determined directly from sampling a series of in-stream piezometers.

3.3 Study Area and Methods

Sixmile Spring and the associated 1st order stream are located in Tooele Valley, approximately 45 km west of Salt Lake City, Utah (Fig. 3.1). The Sixmile System is one of 4 regional groundwater discharge locations at the northern terminal end of the Tooele Valley groundwater basin [*Stolp and Brooks*, 2009]. Average groundwater flow through the basin is about 7.5 x 10^7 m^3/yr; average discharge of the Sixmile System is about 3.5 x 10^6 m^3/yr. The initial 593 m of the Sixmile System was investigated in terms of groundwater inflows and gas exchange.

The investigation of groundwater inflows and gas exchange consisted of the following elements:

- Measure the specific discharge of groundwater to the stream (q, in m/sec),
- Quantify the chloroflourcarbon-12 gas-exchange velocity ($k_{CFC\text{-}12}$, cm/hr),
- Measure the profile of stream water $C_{CFC\text{-}12}$ along the study reach
- Using q and $k_{CFC\text{-}12}$, simulate gas transport to reproduce observed stream water $C_{CFC\text{-}12}$ by adjusting groundwater inflow $C_{CFC\text{-}12}$,
- Sample a set of in-stream piezometers and directly measure groundwater $C_{CFC\text{-}12}$,
- Compare the flow-weighted average groundwater inflow $C_{CFC\text{-}12}$ estimated from simulation of gas transport to the flow-weighted average determined from direct measurements of groundwater $C_{CFC\text{-}12}$.

The specific discharge of groundwater was quantified by injecting a known mass-rate of bromide, ($M_{load,Br}$, in mg/min) into the stream until concentrations along the study reach come to steady state. Steady state was evaluated by collecting a time series of stream samples at the downstream end of the study reach, starting 1-hr after the start of

injection and ending 24-hrs after the end of injection. Once at steady state, the stream was sampled at 10 locations and the observed bromide concentration (C_{Br}, in mg/L) profile used to determine inflow. At 593 m the stream was sampled at 6 discrete points to assess the level of bromide mixing. Samples were analyzed using an ion chromatograph with detection limit of 50 parts per billion (ppb) and an accuracy of about 5% for values greater than 250 ppb. Using the One-Dimensional Transport with Inflow and Storage (OTIS) model [*Runkel*, 1998] a steady-state calibration to the observed C_{Br} profile was obtained by specifying groundwater inflows. The mis-fit between simulated and observed C_{Br} was minimized with UCODE [*Poeter and others*, 2005]. The simulation accounts for background C_{Br}, which is 1 mg/L at Sixmile.

The $k_{CFC\text{-}12}$ was quantified by the same methodology as described for groundwater inflow. Instead of bromide, chloroflourocarbon-12 was injected into the stream by diffusion through silicon tubing and sampled at the same 10 locations. Samples were analyzed using a gas chromatograph at the University of Utah Dissolved Gas Center with detection limit of about 0.005 pmoles/kg and an accuracy of about 3% for values above 0.1 pmoles/kg. Using a modified version of OTIS that includes gas exchange, the observed gas concentrations were simulated by adjusting a gas-exchange coefficient. Specific groundwater inflow for each segment is fixed according to the amounts determined from bromide dilution. The groundwater inflow $C_{CFC\text{-}12}$ does not influence simulation results because it is several orders-of-magnitude less than stream $C_{CFC\text{-}12}$ concentrations created during gas-injection. The gas-exchange coefficient was optimized using UCODE to simulate gas concentrations for the stream water that are a reasonable facsimile of the observed values.

One year after the injections, ambient stream water $C_{CFC\text{-}12}$'s were measured from 8 stream samples collected along the 593 m reach. For stream samples, glass sample-bottles were held under the surface and actively flushed for 90 seconds with a small pump. During collection the samples were not allowed to come into direct contact with the atmosphere.

Using the previously defined gas-exchange coefficient and groundwater-inflow, observed ambient stream water $C_{CFC\text{-}12}$ was simulated using the modified OTIS simulator. A single parameter representing $C_{CFC\text{-}12}$ of inflowing groundwater was adjusted to minimize the mis-fit between simulated and observed stream water $C_{CFC\text{-}12}$; optimization was done using UCODE. Because groundwater inflow is incorporated into the simulation, the solution represents the flow-weighted average $C_{CFC\text{-}12}$.

In conjunction with ambient stream sampling, groundwater was also sampled from 10 piezometers completed at various depths and locations along the study reach (Fig. 3.2). For piezometers with water levels below the stream-air interface, samples were collected using a peristaltic pump equipped with tubing having a low gas permeability. For piezometers with water levels above the interface (flowing), water was routed through copper tubing into a bucket from which samples were collected. Using the C_{Br} determined q, the $C_{CFC\text{-}12}$'s measured for individual piezometers are flow-weighted as:

$$C_{CFC-12} = \sum_{i=1}^{n} (C_{CFC-12_i} * q_i) \Big/ \sum_{i=1}^{n} q_i \qquad (1)$$

The q_i attributed to individual piezometers was assigned in accordance to location within the q_i profile of the stream. The validity of gas-exchange corrected stream-water

C_{CFC-12} is measured by how similar it is to the direct measurement of groundwater C_{CFC-12}.

3.4 Results

Tracer tests, piezometer installation, and water sampling experiments at Sixmile were done between July 2005 and August 2006. During bromide injection, steady-state conditions along the stream were reached in about 9-hours. The C_{Br} profile ranged from 4.5 to 2.3 mg/L and identified 54.6 (L/sec) of groundwater inflow (Table 3.1). During CFC-12 injection, concentrations varied from 31,792 pmoles/kg at 50 m to 10,594 pmoles/kg at 593 m (Table 3.1); the computed k_{CFC-12} is 0.48 m/day. In May-September 2006 stream water C_{CFC-12} ranged from 0.91 to 1.37 (pmoles/kg) and groundwater C_{CFC-12} concentrations of samples collected at 10 piezometers ranged from 0.31 to 1.39 pmoles/kg (Table 3.1). The flow-weighted average groundwater inflow C_{CFC-12} is 1.16 pmoles/kg; the flow-weighted piezometer derived groundwater inflow C_{CFC-12} is 1.08 pmoles/kg. A simple average of stream water C_{CFC-12} is 1.22 pmoles/kg.

3.5 Interpretation

The determination of groundwater inflow and q was done using OTIS to simulate the observed C_{Br} profile along the study reach (Fig. 3.3). The minimum mis-fit to observed conditions was achieved with UCODE. Initially 9 inflow amounts (a stream segment between each of the observation locations) were adjusted to fit the 10 C_{Br} observations. This approach results in an excellent fit to the observations but the 95% confidence interval is large. The 95% confidence interval is a statistic that is related to the number of observations (C_{Br}) used to determine a parameter value (groundwater inflow).

When the ratio of observations to parameters is essentially 1, confidence that the parameter value is similar to the "true" value, is not high. On the basis of area-velocity discharge measurements that indicate 2/3 of inflow occurs along the upper 350 m of the study reach, the stream discretization was reduced from 9 segments to 2 segments (0 to 350 m and 350 to 593 m). The resulting inflows and 95% confidence intervals are 1.6 x 10^{-4} m^3/sec-m (1.2 x 10^{-4} to 2.0 x 10^{-4} m^3/sec-m) and 3.1 x 10^{-5} m^3/sec-m (0.0 to 1.3 x 10^{-5} m^3/sec-m). The 95% confidence intervals is an interval statistic that implies if a series of Br injections were conducted at Sixmile under identical hydrologic conditions, 95% of those hypothetical tests would quantify an inflow that falls within the 95% CI. Using a stream width and length, q for the 2 segments are 1.2 x 10^{-4} to 1.1 x 10^{-5} m/sec, respectively. Total estimated inflow to the Sixmile System is estimated at 82.9 L/sec, 28.3 L/sec from the spring orifice and 54.6 L/sec as groundwater inflow below the spring.

The estimated $k_{CFC\text{-}12}$ at Sixmile was derived by dissolving chloroflourocarbon-12 into the stream water at 4 orders of magnitude above background. Although high stream concentrations were obtained, the amount of gas released into the environment was estimated at less than 100 grams. Using 10 $C_{CFC\text{-}12}$ observations, the modified version of OTIS was used to determine a single gas-exchange coefficient for the study reach. As with groundwater $C_{CFC\text{-}12}$, a better match to observations can be obtained by assigning coefficients to individual stream segments, but the level of confidence in the values become marginal. Using a single parameter, the lowest sum of squared residuals obtained by UCODE occurs with a gas-exchange coefficient of 3.0 x 10^{-5} sec^{-1} with a 95% confidence interval of 0.9 x 10^{-5} to 1.4 x 10^{-5} sec^{-1} (Fig. 3.4). When multiplied by an average stream depth of .185 m the gas-exchange velocity for the Sixmile System is 5.6 x

10^{-6} m/sec.

To derive the flow-weighted groundwater inflow C_{CFC-12}, a final OTIS simulation was performed using previously estimated groundwater inflows and gas-exchange coefficient. Inflow C_{CFC-12} is adjusted to minimize the mis-fit between observed and simulated stream-water C_{CFC-12}. Using a single parameter to describe inflow for the entire stream reach, a concentration of 1.16 pmoles/kg gave the best fit to observed conditions. The 95% CI is 0.94 to 1.37 pmoles/kg (Fig. 3.5). This derived inflow concentration is in close agreement with the 1.08 pmoles/kg determined from direct sampling of groundwater at 13 piezometers (Table 3.1). The piezometer estimate is biased to the upper 250 m of the study reach, from which 12 of the 13 samples were collected. The upper piezometer values were flow weighted using 1.2×10^{-4} m/sec, the lower-reach piezometer was weighted using 1.1×10^{-5} m/sec.

The ambient stream-water C_{CFC-12}'s in August 2006 were significantly less than the air-equilibration value of 2.25 pmoles/kg along the entire 593 m study reach (Fig. 3.5). The degree to which stream-water concentrations are not at air-equilibration suggests that the groundwater signal can be recovered with a high level of certainty. Just the simple average of stream water C_{CFC-12}, 1.22 pmoles/kg, gives an answer within the 95% CI, without any consideration of gas-exchange, and is only 0.14 pmoles/kg above the groundwater concentration measured in the piezometers. The k_{CFC-12}/q ratio is a measure how successfully the groundwater signal can be recovered. At Sixmile the ratio is 0.13, which means the processes that contribute to loss of a groundwater signal are almost an order of magnitude weaker that those that create the signal. This is evident by both the degree that ambient stream-water C_{CFC-12}'s are below air equilibration and the

nearly constant concentration profile of the reach (Fig. 3.5).

The concept of k/q is generalized in Fig. 3.6, where groundwater concentration and resulting stream-water concentration (both normalized to the air-equilibrated concentration) are plotted as a function of k/q. The k/q lines are generated by OTIS using generic values of k and q. The critical factor controlling the slopes is the relative differences between k and q (expressed in the ratio), not the absolute values of k and q.

3.6 Conclusions

The experiment at Sixmile was designed to evaluate methods of determining the concentration of dissolved gases of waters that emerge from natural discharge locations. The gas concentrations are a flow-weighted average for the contributing area and can be used to quantify groundwater storage. The complicating factor is that dissolved gases are nonconservative at natural discharge locations, where groundwater becomes exposed to the atmosphere.

The experiment consisted of measuring discharge and the gas-exchange velocity and stream-water $C_{CFC\text{-}12}$. That information was then used to simulate gas transport and the flow-weighted groundwater inflow $C_{CFC\text{-}12}$. The simulated groundwater concentration was nearly identical to the concentrations measured in and averaged from 13 piezometers located along the study reach. Although results support the efficacy of the method, the experiment is not a robust measure for all streams. This is due to the extremely favorable conditions at the Sixmile System in which the stream is so strongly gaining. The most important conclusion from the experiment is that groundwater gas concentrations are essentially equivalent to stream concentrations when the processes affecting loss of the gas signal are nearly an order of magnitude less than those creating the signal. The

conditions at Sixmile are not common for most gaining stream reaches, but are very likely at distinct spring orifices.

3.7 References

P. G. Cook and J. K. Böhlke, (2000), Determining the timescales for groundwater flow and solute transport, in *Environmental Tracers in Subsurface Hydrology*, edited by P. G. Cook and A. L. Herczeg, Kluwer Acad. Publ., Boston, Mass.

Poeter, E. E., M. C. Hill, E. R. Banta, S. W. Mehl, and S. Christensen, (2005), UCODE-2005 and six other computer codes for universal sensitivity analysis, calibration, and uncertainty evaluation; constructed using the JUPITER API, *U.S. Geol. Surv. Tech. and Meth. 6-A11*, 283 p.

Runkel, R. L., (1998), One-dimensional transport with inflow and storage (OTIS): A solute transport model for streams and rivers, *U.S. Geol. Surv. Water Resour. Invest. Rep. 98-4018*, 70 p.

Stolp, B. J., and L. E. Brooks, (2009), Hydrology and simulation of ground-water flow in the Tooele Valley ground-water basin, Tooele County, Utah, *U.S. Geol. Surv. Scien. Invest. Rep. 2009-5154*, 86 p., 3 appendices, 1 pl. Available at http://pubs.usgs.gov/sir/2009/5154/.

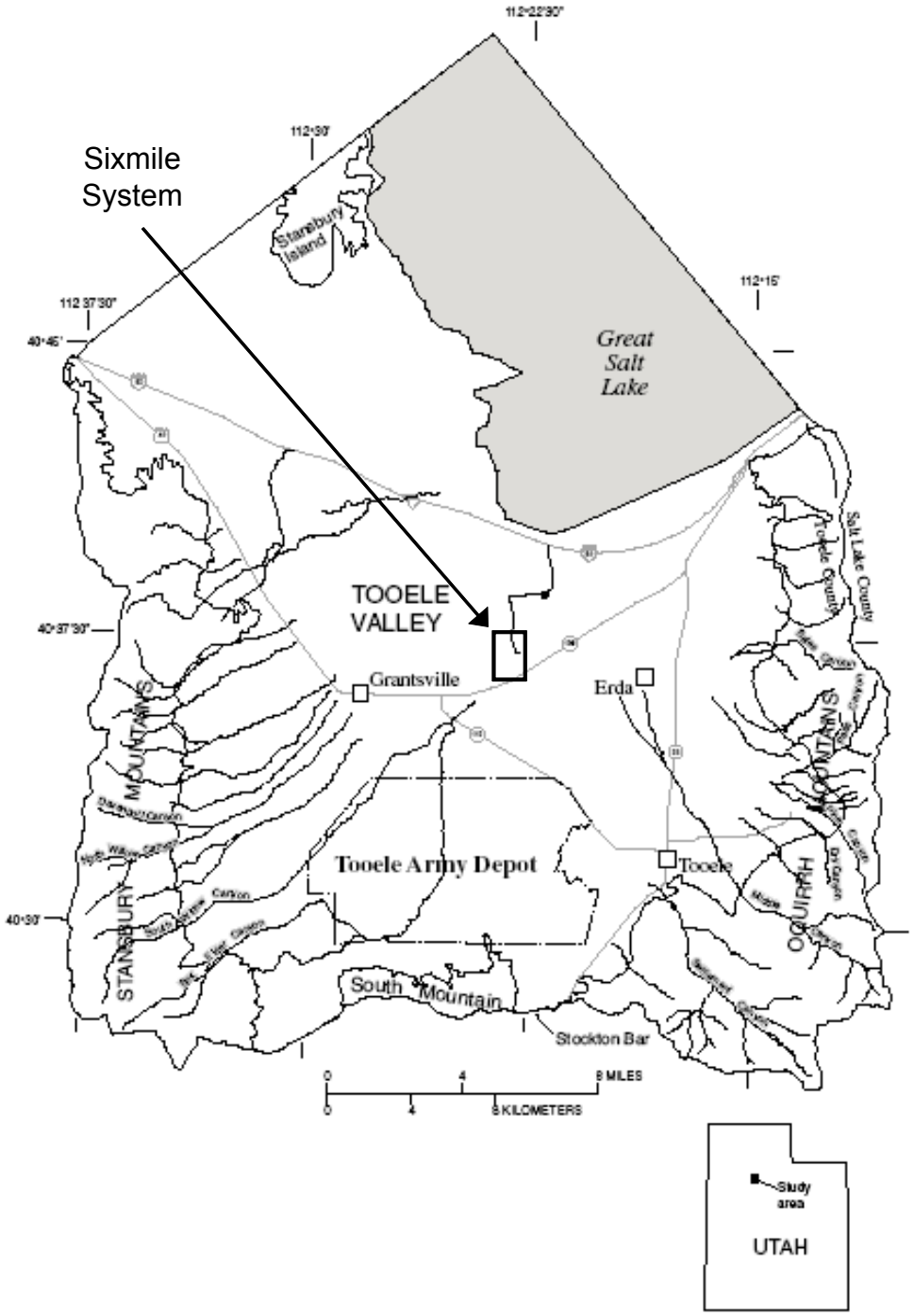

Figure 3.1 Location of the Sixmile System within the Tooele Valley groundwater basin, Tooele County, Utah.

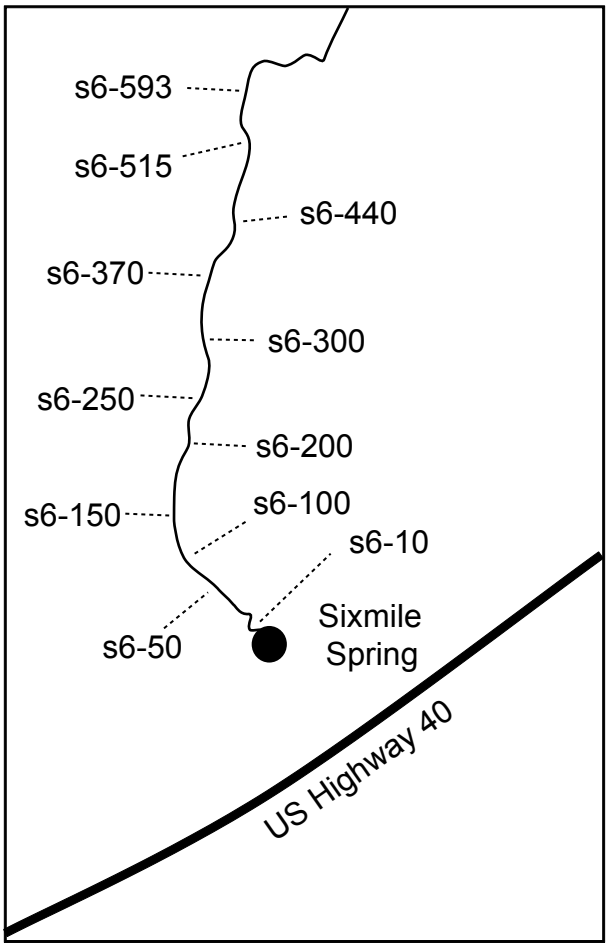

Figure 3.2 Sample locations at the Sixmile System, Tooele County, Utah.

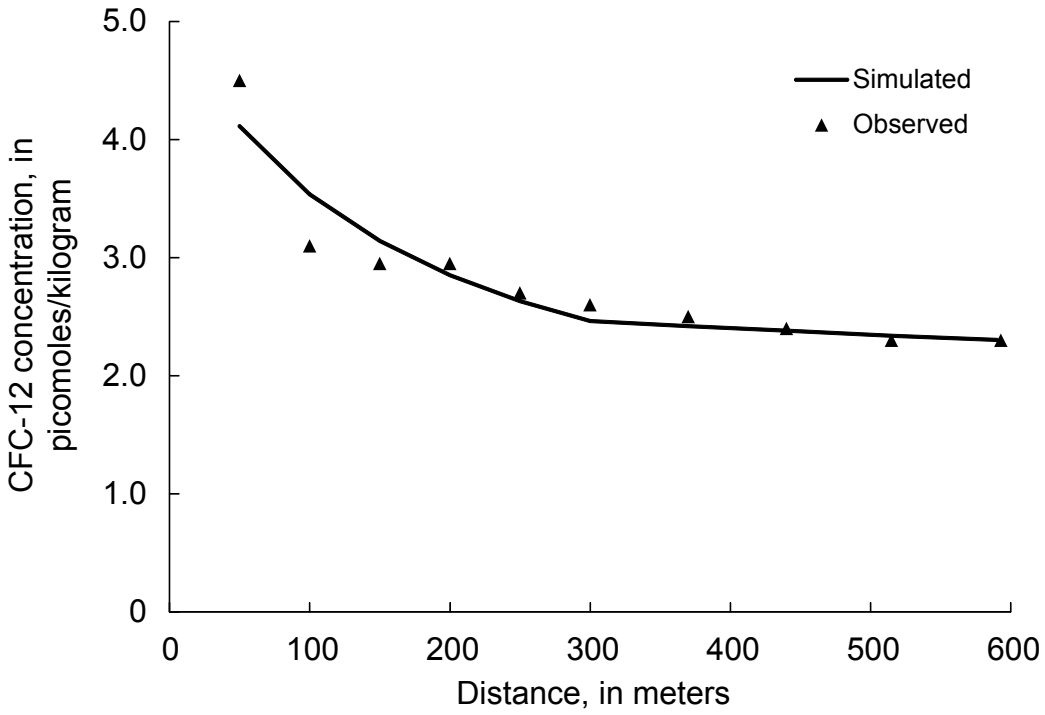

Figure 3.3 Observed and simulated bromide concentration profiles during solute-tracer injection at the Sixmile System, Tooele County, Utah.

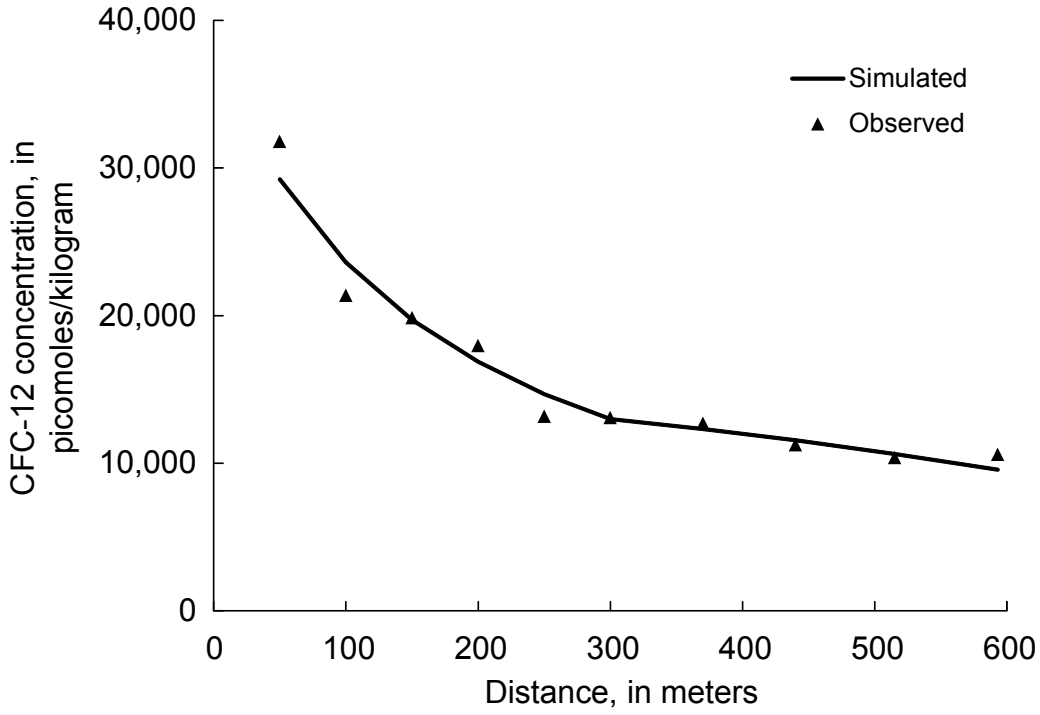

Figure 3.4 Observed and simulated chloroflourocarbon-12 concentration profiles during gas-tracer injection at the Sixmile System, Tooele County, Utah.

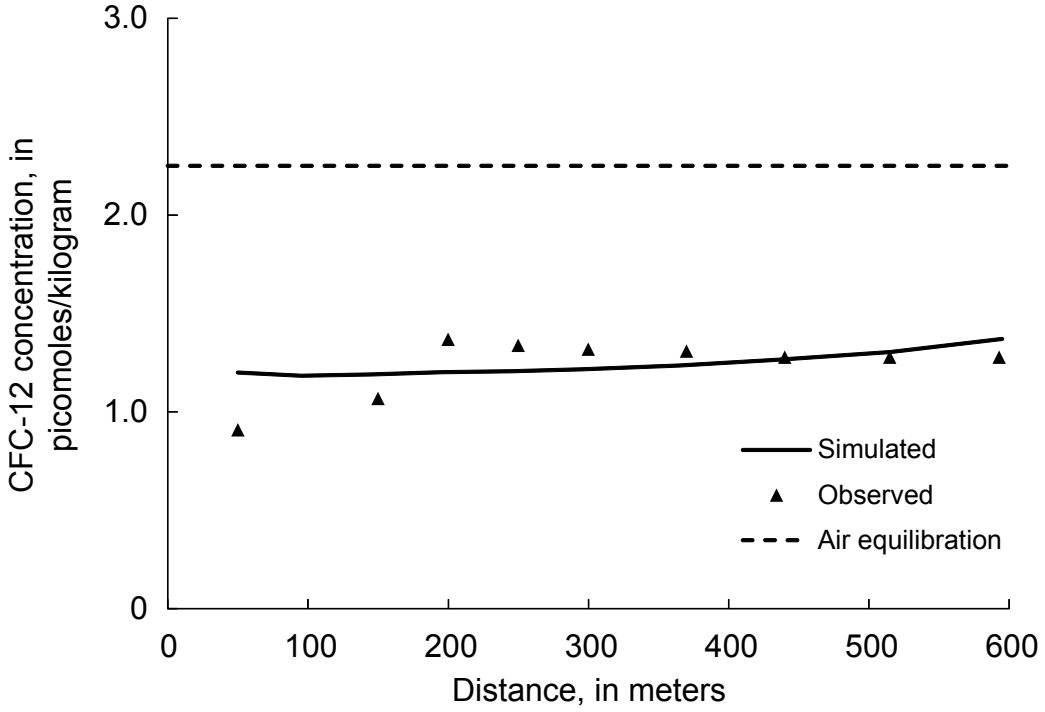

Figure 3.5 Observed and simulated chloroflourocarbon-12 concentration profiles at the Sixmile System, Tooele County, Utah.

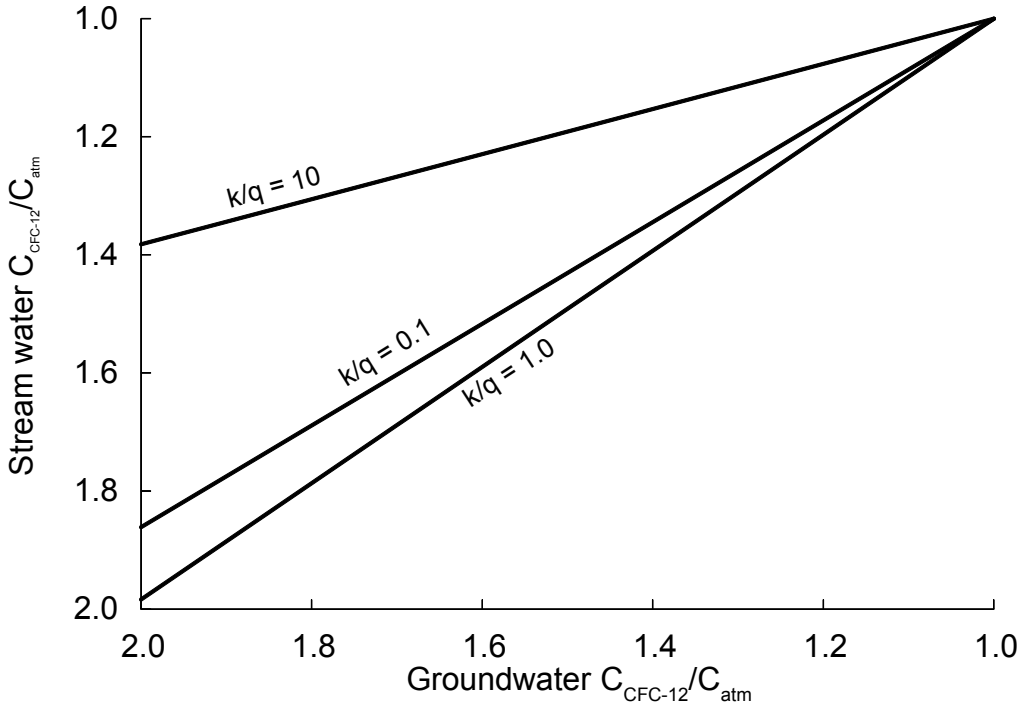

Figure 3.6 The relationship between the concentration of a dissolved gas in groundwater and stream water as a function of k/q.

Table 3.1 Sample site locations, piezometer information, bromide concentrations, and chloroflourocarbon-12 concentrations at the Sixmile System, Tooele County, Utah.

Site ID	Location NAD83 UTM zone 12 latitude	Location NAD83 UTM zone 12 longitude	Distance from spring (m)	Sample type	Piezometer ID	Piezometer depth (m)	Sample date	Bromide (mg/L)	CFC-12 (picomoles/kg)	Comment
s6-0	4,496,329	382,922	0	ambient stream CFC-12			8/31/2006	- -	1.20	1 bottle
				piezometer	PVC-1	0.6	5/10/2006	- -	1.39	average of 2 bottles
				piezometer	PVC-1		9/7/2006	- -	1.38	average of 3 bottles
s6-10	4,496,339	382,897		Injection site				- -	- -	injectate sample only
s6-50	4,496,369	382,860	50	injection stream bromide			7/28/2005	4.5	- -	grab sample
				injection stream CFC-12			7/28/2005	- -	31,792	
				ambient stream CFC-12			8/31/2006	- -	1.17	average of 3 bottles
				ambient stream CFC-12			- -	- -	0.91	average of 3 bottles
				ambient piezometer CFC-12	PVC-2	0.6	- -	- -	- -	
s6-100	4,496,417	382,834		injection stream bromide			7/28/2005	3.1	- -	grab sample
				injection stream CFC-12			7/28/2005	- -	21,366	
s6-150	4,496,454	382,832	150	injection stream bromide			7/28/2005	2.95	- -	grab sample
				injection stream CFC-12			7/28/2005	- -	19,849	
				ambient stream CFC-12			8/31/2006	- -	1.07	1 bottle
				ambient piezometer CFC-12	PVC-3west	0.6	5/10/2006	- -	1.07	average of 2 bottles
				ambient piezometer CFC-12	PVC-3west		9/4/2006	- -	1.16	average of 2 bottles
				ambient piezometer CFC-12	PVC-3middle	0.6	5/10/2006	- -	1.04	average of 2 bottles
				ambient piezometer CFC-12	PVC-3middle		9/7/2006	- -		
				ambient piezometer CFC-12	metal-7west	2.0	9/4/2006	- -	1.11	average of 3 bottles
				ambient piezometer CFC-12	metal-7middle	2.0	9/4/2006	- -	1.35	average of 3 bottles
				ambient piezometer CFC-12	metal-7east	2.0	9/4/2006	- -	1.15	average of 3 bottles
				ambient piezometer CFC-12	metal-14west	4.0	- -	- -	- -	
				ambient piezometer CFC-12	metal-14middle	4.0	- -	- -	- -	
				ambient piezometer CFC-12	metal-14east	4.0	- -	- -	- -	
				ambient piezometer CFC-12	metal-21middle	6.0	9/4/2006	- -	0.32	average of 3 bottles
				ambient piezometer CFC-12	metal-21east	6.0	8/31/2006	- -	0.31	average of 3 bottles
s6-200	4,496,511	382,846	200	injection stream bromide			7/28/2005	2.95	- -	integrated sample
				injection stream CFC-12			7/28/2005	- -	17,956	
				ambient stream CFC-12			8/31/2006	- -	1.37	average of 3 bottles
				ambient piezometer CFC-12	PVC-4	0.6	5/10/2006	- -	0.62	average of 2 bottles
				ambient piezometer CFC-12	PVC-4	0.6	9/7/2006	- -	0.81	average of 3 bottles
s6-250	4,496,566	382,856	250	injection stream bromide			7/28/2005	2.7	- -	integrated sample
				injection stream CFC-12			7/28/2005	- -	13,185	
				ambient stream CFC-12			8/31/2006	- -	1.34	average of 3 bottles
				ambient piezometer CFC-12	PVC-5	0.6	5/10/2006	- -	1.24	average of 2 bottles
				ambient piezometer CFC-12	PVC-5	0.6	9/7/2006	- -	1.44	average of 3 bottles
s6-300	4,496,613	382,862	300	injection stream bromide			7/28/2005	2.5	- -	integrated sample
				injection stream CFC-12			7/28/2005	- -	13,089	
				ambient stream CFC-12			8/31/2006	- -	1.32	average of 3 bottles
				ambient piezometer CFC-12	PVC-6	0.6	- -	- -	- -	possible H2S
s6-370	4,496,685	382,877	370	injection stream bromide			7/28/2005	2.4	- -	integrated sample
				injection stream CFC-12			7/28/2005	- -	12,692	
				ambient stream CFC-12			8/31/2006	- -	1.32	average of 3 bottles
				ambient piezometer CFC-12	PVC-7	0.6	- -	- -	- -	
s6-440	4,496,721	382,897		injection stream bromide			7/28/2005	2.3	- -	integrated sample
				injection stream CFC-12			7/28/2005	- -	11,240	
s6-515	4,496,789	382,895	515	injection stream bromide			7/28/2005	2.3		integrated sample
				injection stream CFC-12			7/28/2005	- -	10,390	
				ambient stream CFC-12			8/31/2006	- -	1.28	average of 3 bottles
				ambient piezometer CFC-12	PVC-8	0.6	5/10/2006	- -	0.71	average of 2 bottles
				ambient piezometer CFC-12	PVC-8		8/31/2006	- -	0.89	1 bottle
s6-593	4,496,859	382,907		injection stream bromide			7/28/2005	2.3	- -	integrated sample
				injection stream CFC-12			7/28/2005	- -	10,594	integrated sample

CHAPTER 4

AGE DATING BASE FLOW AT SPRINGS AND GAINING STREAMS USING HELIUM-3 AND TRITIUM: FISCHA-DAGNITZ SYSTEM, SOUTHERN VIENNA BASIN, AUSTRIA

Stolp, B. J., D. K. Solomon, A. Suckow, T. Vitvar, D. Rank, P. K. Aggarwal, and L. F. Han (2010), Age dating base flow at springs and gaining streams using helium-3 and tritium: Fischa-Dagnitz system, southern Vienna Basin, Austria, Water Resour. Res., 46, W07503, doi:10.1029/2009WR008006.

WATER RESOURCES RESEARCH, VOL. 46, W07503, doi:10.1029/2009WR008006, 2010

Age dating base flow at springs and gaining streams using helium-3 and tritium: Fischa-Dagnitz system, southern Vienna Basin, Austria

B. J. Stolp,[1] D. K. Solomon,[1] A. Suckow,[2,3] T. Vitvar,[2] D. Rank,[3] P. K. Aggarwal,[2] and L. F. Han[2]

Received 20 March 2009; revised 12 January 2010; accepted 1 February 2010; published 3 July 2010.

[1] Springs and gaining streams are locations where groundwater flow paths naturally converge and discharge as a flow-weighted mixture of water from the contributing aquifer. The age of that water is therefore a good measure of the mean transit time (MTT) of the contributing aquifer. The question examined in this paper is whether tritiogenic helium-3 and tritium ($^3He_{trit}$–^3H) can be used to estimate MTT in these settings. To answer that question two factors must be considered: (1) the loss of ^3He from discharging groundwater as it becomes exposed to the atmosphere, and (2) the accuracy with which MTT can be determined from flow-weighted $^3He_{trit}$–^3H concentrations. These concepts were tested at the Fischa-Dagnitz system (springs and emerging stream), which is part of the southern Vienna Basin aquifer. Conducting a gas tracer test, gas exchange coefficients (λ) were established for helium-4 (^4He) and krypton-84 (^{84}Kr), and derived for helium-3 (^3He) and neon-20 (^{20}Ne). By simulating measured groundwater inflow and gas transport in the stream, groundwater inflow concentrations for ^3He, ^4He, ^{20}Ne, and ^{84}Kr were estimated. Correcting for the various sources of He, the tritiogenic helium-3 ($^3He_{trit}$) concentration of inflowing groundwater was estimated at 8.3 tritium units (TU). The flow-weighted groundwater concentration of ^3H, determined from 22 stream water samples, was estimated at 9.8 TU. Assuming that the relationship between flow amount and transit time at Fischa-Dagnitz is characterized by a hybrid dispersion–exponential age model, the $^3He_{trit}$–^3H ratio (8.3/9.8 = 0.85) defines a MTT of 8 years. The validity of this estimate was evaluated by comparison to a long-term ^3H time series that exists for Fischa-Dagnitz. The likely range of MTT's derived from the measured ^3H time series is 11 to 14 years.

Citation: Stolp, B. J., D. K. Solomon, A. Suckow, T. Vitvar, D. Rank, P. K. Aggarwal, and L. F. Han (2010), Age dating base flow at springs and gaining streams using helium-3 and tritium: Fischa-Dagnitz system, southern Vienna Basin, Austria, *Water Resour. Res.*, *46*, W07503, doi:10.1029/2009WR008006.

1. Introduction

[2] A fundamental description of groundwater flow is mean transit time (MTT). MTT is defined as the average travel time required for water to move from areas of recharge to areas of discharge. MTT is a robust attribute of a groundwater system [*Haitjema*, 1995] that is correlated to the evolution of water quality, resilience to climatic variations, and the development of best management practices. Equally important, MTT is directly related to the rate of recharge and storage volume in an unconfined aquifer [*Cook and Böhlke*, 2000]. Seasonal changes in water levels and streamflow describe groundwater system response to changes in fluid flow. These changes can then be converted into estimates of fluid flux and storage volume if aquifer characteristics are well constrained. On the other hand, MTT is directly related to fluid flow and storage volume. Understanding flow and storage is particularly useful for allocation and prioritization of water resources. The difficulty in quantifying MTT is collecting and successfully dating water samples that represent a reasonable flow-weighted mixture of all flow paths that exist within the aquifer.

[3] At locations where flow paths naturally converge and discharge to the surface, the water is a flow-weighted mixture of all flow paths that exist in the contributing aquifer. Groundwater age of the mixture quantifies a mean time that it takes for water to move through the contributing aquifer. Locations of converging flow paths include springs and gaining streams. Potential approaches to derive the age of water at natural discharge areas include (1) ^3H time series, (2) stable isotope time series, and (3) age dating tracers such as CFCs, SF_6, and the $^3He_{trit}$–^3H ratio. When the temporal variability of ^3H in precipitation (aquifer recharge) can be compared with temporal patterns of ^3H in spring and stream water at base flow, the offset in discernible events like the 1963 ^3H peak is a powerful way of evaluating MTT [*Dincer et al.*, 1974]. This requires time series for both recharge and discharge; unfortunately relatively few of these coupled ^3H

[1]Geology and Geophysics Department, University of Utah, Salt Lake City, Utah, USA.
[2]Isotope Hydrology Section, International Atomic Energy Agency, Vienna, Austria.
[3]Center for Earth Sciences, University of Vienna, Vienna, Austria.

0043-1397/10/2009WR008006

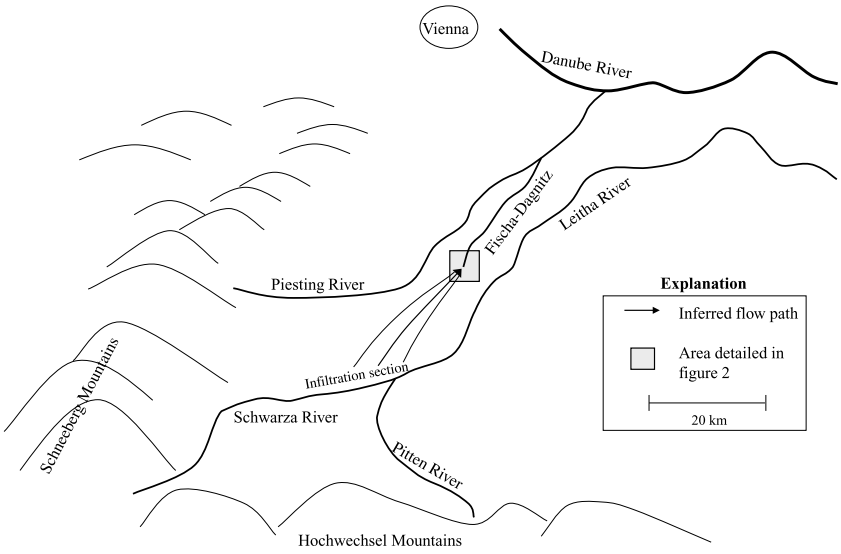

Figure 1. Diagram showing the general hydrology of the southern Vienna Basin.

time series exist. The seasonal variation of stable isotopes of hydrogen and oxygen in precipitation can also be measured in streams and potentially provide a method for estimating MTT. However, longitudinal dispersion tends to average out input periodicity making it increasingly difficult to derive MTTs greater than 3 to 5 years. *McGuire and McDonnell* [2006] present a comprehensive review of techniques and issues associated with estimating transit times for catchments.

[4] Even if an ideal tracer existed (one that accumulates in groundwater at a uniform rate and is chemically inert [*Kazemi et al.*, 2006]), determining the travel time of a flow-weighted mixture of water (and thereby MTT) is inherently complex. Although not ideal, groundwater dating using dissolved gases has become relatively common in recent years [*Busenberg and Plummer*, 1992; *Cook and Solomon*, 1997; *Solomon and Cook*, 2000]. When water is exposed to the atmosphere (as occurs at natural discharge areas) the dissolved gases in the water begin to equilibrate toward atmospheric concentrations. If gas exchange across the air-water interface is rapid, groundwater discharging to the spring or stream would fully equilibrate with the atmosphere and have a "modern" apparent age. Alternatively, if exchange is slow, a gas signal that represents groundwater inflow will be present in spring and stream water (see Appendix A1). The effects of gas equilibration (exchange) can be quantified by simulating gas transport using one-dimensional advection/dispersion. Boundary conditions include the dissolved-gas inflow concentrations (via groundwater) and gas exchange across the water/air interface.

[5] Another aspect of dating mixed water is that if the relationship between concentration and age (i.e., the age equation) is nonlinear, then using the arithmetic mean concentration (although flow-weighted) of the tracer in the age equation will not give the mean age. This condition is true regardless of other nonlinearities created by the tracer input function (e.g., the ^{3}H bomb peak) or the age structure within the aquifer (e.g., dispersion or exponential distribution of age). The discrepancy between MTT and mean apparent age (derived from the age equation using the mean concentration) is minor when the range of travel times in the aquifer is small. Most age equations can be reasonably approximated by a linear function over short time intervals. The discrepancy becomes more significant as the range of travel times (and nonlinearity) increases.

[6] The central question examined in this paper is whether $^3He_{trit}$ and ^{3}H concentrations in well-mixed spring/stream water can be used to make a meaningful estimate of the MTT in the contributing groundwater system. We investigated this at Fischa-Dagnitz where a long-term time series of ^{3}H concentrations provides an independent appraisal of MTT.

2. Study Area

[7] The Fischa-Dagnitz system consists of three distinct springs, located within about 200 m of each other, and the first-order stream that begins at the springs. There is no existing stream channel upgradient of the springs and no perennial or obvious ephemeral stream tributaries along the study reach. The stream eventually flows into the Piesting River (Figure 1). The spring and stream are part of the southern Vienna Basin aquifer, and are located approximately 35 km south of Vienna, Austria. Previous authors [*Rank and Papesch*, 2003] suggest that recharge for the spring is infiltration from the Schwarza River, located about 20 km to the south (Figure 1). Infiltration is into a gravel deposit that is of sufficient permeability that the Schwarza River does not flow beyond the infiltration section during summer, fall and winter months. Infiltration includes snow-melt runoff (in the spring) along the entire infiltration reach and base flow (in late summer, fall, and winter) along the upper end of the infiltration reach. Near and to the north of the Fischa-Dagnitz system perennial flow exists in various

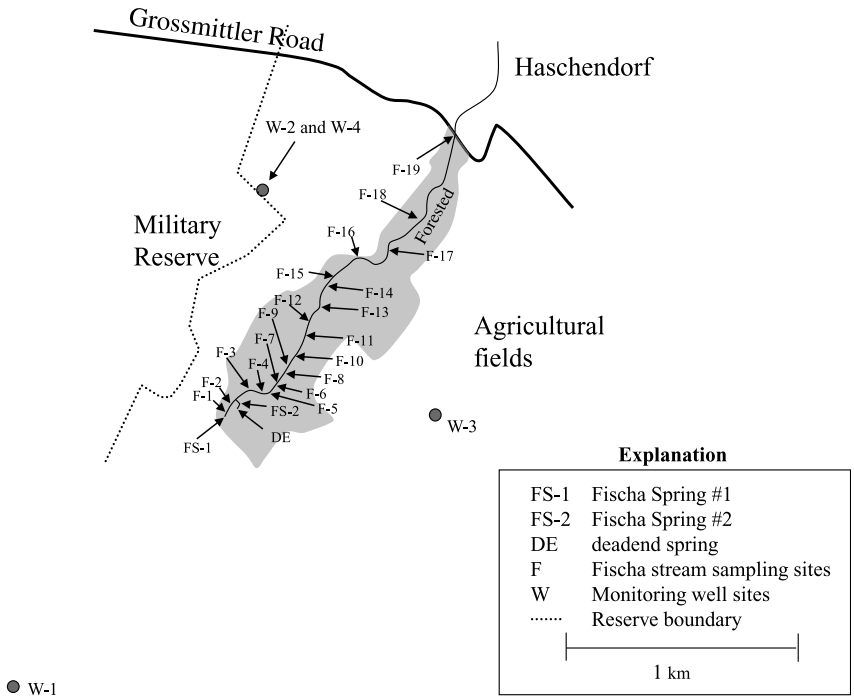

Figure 2. Sampling and discharge measurement locations in the Fischa-Dagnitz system.

gaining streams including the Leitha River (Figure 1). This analysis of the Fischa-Dagnitz contributing aquifer includes a spatially distributed recharge component that originates from precipitation and irrigation within the southern Vienna Basin.

3. Methods

[8] Assigning a $^{3}He_{trit}$–^{3}H based MTT to water issuing from springs and along strongly gaining streams is a multi-step process. Initially water and gas samples must be collected at orifices and/or along the gaining stream. Next, the gas exchange characteristics for the stream need to be established by conducting a gas tracer test. Once exchange coefficients are known, the stream water concentrations are corrected for exchange with the atmosphere. The corrected concentrations are assumed to represent the flow-weighted mean of groundwater discharging at the spring or gaining stream. The last step consists of assigning a transit time distribution to the contributing aquifer, which is based on recharge-discharge geometry. The MTT of the transit time distribution is then adjusted until a reasonable match between simulated and estimated $^{3}He_{trit}$ and ^{3}H concentrations is achieved. Overall error in MTT comes from uncertainty associated with estimating concentrations and the transit time distribution within the contributing aquifer.

[9] In Fall 2006, dissolved-gas samples were collected from the Fischa-Dagnitz system and nearby monitoring wells to quantify the naturally occurring concentrations of ^{3}He, ^{4}He, nitrogen (N_2), neon (^{20}Ne), argon (^{40}Ar), and krypton (^{84}Kr); sample locations are shown in Figure 2. The sample reach extends from Fischa Spring (FS-1) to the bridge at Grossmittler Road (F-19), and is 1,899 m long. Gas samples were collected using passive diffusion samplers. Samplers were suspended at the approximate center of the water column and allowed to equilibrate; equilibration takes about 24 h. Temperature, total dissolved gas pressure, and dissolved oxygen were measured at sample locations using a HydroLab 4a sonde. In conjunction with gas sampling, stream water was collected in 500 ml bottles for analysis of ^{3}H.

[10] Groundwater inflow was quantified by measuring stream discharge at numerous locations along the study reach. An Acoustic Doppler Velocimeter (ADV) was used to measure the average streamflow velocity at 4/10th distance up from the stream bottom. At each discharge location the stream was subdivided into 20 to 25 vertical sections and a velocity measured for each vertical section. A cross-sectional area was assigned to each section on the basis of stream depth and distance between successive sections. Stream discharge was obtained by summing the flow (velocity * area) for all vertical sections. Groundwater inflow was calculated as the difference in streamflow between successive discharge measurements.

[11] Gas exchange characteristics for Fischa-Dagnitz were determined by injecting He and Kr into the stream. The gases were plumbed via nylon tubing (which has a low gas diffusion coefficient) through a flowmeter to the stream. At the stream, the gas was routed through silicone tubing (which has a high gas diffusion coefficient) placed on the stream bottom. Additional nylon tubing was attached to the end of the silicone tubing to route gas back from the stream to a valve

that created backpressure. Beyond the valve gas was vented to the atmosphere. Venting creates flow through the tubing and flushes out any back-diffused gases from the stream. The gas flow-through rate averaged 20 cm^3/sec. Using silicone tubing with an outside diameter of 9.5 mm and a wall thickness of 3.2 mm, tubing lengths of 1.8 and 5.3 m were used for He and Kr, respectively. Lengths were calculated using Fick's first law and estimated values of 4.3 e-8 and 3.2 e-7 m^2/sec for the effective diffusion coefficient of He and Kr in silicone. The effective diffusion coefficient is the product of the solubility of a gas into silicone and the molecular diffusion of gas through silicone. Tubing length and backpressure were designed to increase He and Kr by about 1 order of magnitude above air-equilibration values.

[12] Atmospheric exchange of the elevated concentrations of He and Kr was simulated with a modified version of the One-dimensional Transport with Inflow and Storage (OTIS) model [*Runkel*, 1998]. The modified version simulates gas exchange across the air-water interface as a first-order process:

$$\frac{dC_{str}}{dt} = \lambda(C_{atm} - C_{str-simulated}) \quad (1)$$

where λ [1/t] is the gas exchange coefficient [*Wanninkhof et al.*, 1990], C_{atm} [L^3/M] is the air-equilibrated gas concentration, and $C_{str\text{-}simulated}$ is the simulated gas concentration in the stream. The stream was discretized into segments that correspond to distances between successive discharge measurements. Groundwater inflow was assigned to each segment in accordance with estimated groundwater inflow amounts. All other model parameters were varied for the stream as a whole; parameters were not adjusted for individual segments. Model parameters that affect $C_{str\text{-}simulated}$ are lambda (λ) and the gas concentration of inflowing groundwater (C_{in}). Elevated gas concentrations created by injection reduce OTIS sensitivity to C_{in} and increase sensitivity to λ. To that end a rough estimate of C_{in} was made (it has little effect on calibration to the elevated gas tracer concentrations) and fixed in the model. Lambda was adjusted until a reasonable match between $C_{str\text{-}simulated}$ and the measured gas concentrations in the stream ($C_{str\text{-}measured}$) were obtained. The match was measured as:

$$sigma = \frac{\left(\sum_{i=1}^{n_{sample}} (C_{str-measured_i} - C_{str-simulated_i})^2\right)^{0.5}}{n_{sample}} \quad (2)$$

[13] Gas concentration is in ccSTP/g and n_{sample} is the number of sample sites. Using the elevated gas concentrations, λ's were estimated for the isotopes ^{4}He and ^{84}Kr.

[14] Using λ's for ^{4}He and ^{84}Kr, the gas-exchange mechanisms for Fischa-Dagnitz were computed. The following relationship between the λ's and aqueous diffusion coefficients (D[L^2/t]) [*Jähne et al.*, 1987] was assumed:

$$\frac{\lambda_{4_{He}}}{\lambda_{84_{Kr}}} = \left(\frac{D_{4_{He}}}{D_{84_{Kr}}}\right)^n \quad (3)$$

[15] The D's were corrected for the temperature of stream water [*Jähne et al.*, 1987]. The exponent n[unitless] can range from 0.5 to 1.0 and describes the role of turbulent flow and diffusion exchange across the air-water interface. A value of 0.5 describes exchange dominated by turbulent flow; a value 1.0 describes exchange by molecular diffusion. Intermediate values of n indicate that both mechanisms contribute to exchange. Solving for n using ^{4}He and ^{84}Kr, a form of equation (3) (specific to Fischa-Dagnitz) was then used to determine λ's for ^{3}He and ^{20}Ne.

[16] After λ's were quantified, the modified version of OTIS was used for a second objective, which is determining the ^{3}He, ^{4}He, ^{20}Ne, and ^{84}Kr concentrations of inflowing groundwater. Note that C_{in} values for ^{4}He and ^{84}Kr used in the gas tracer test simulations are rough estimates that have little effect on the determination of λ's. Model discretization for the second objective (determining C_{in}'s) is the same as assigned for the gas tracer simulations. The fundamental difference for the second objective is that λ's were held constant at values determined from the gas tracer test. Further C_{in}'s were adjusted to minimize the difference between simulated and naturally occurring (measured) gas concentrations in stream water. The C_{in}'s of ^{3}He, ^{4}He, ^{20}Ne, and ^{84}Kr are then used to estimate $^3He_{trit}$ with the atmospheric excess-air component derived from the Closed system Equilibrium (CE) model [*Aeschbach-Hertig et al.*, 2000]. In conjunction with ^{3}H measured directly from stream water, a $^3He_{trit}$–^{3}H ratio can be calculated for the flow-weighted mixture of groundwater that exists in the stream.

[17] Gas samples collected prior to and during injection were analyzed at the University of Utah Dissolved Gas Center with replicate samples processed at the Isotope Hydrology Laboratory of the International Atomic Energy Agency (IAEA). Extracted gases were inlet to a cryogenic and chemical getter cleanup system followed by analysis using a sector-field mass spectrometer for helium isotopes and a quadrupole mass spectrometer for ^{20}Ne, ^{40}Ar, and ^{84}Kr isotopes. Tritium samples were analyzed at the Isotope Hydrology Laboratory of the IAEA.

4. Results

[18] Naturally occurring ^{3}He and ^{4}He concentrations (prior to the gas tracer test) along the Fischa-Dagnitz system were measured at 9 locations. Excluding samples collected directly from the springs, gas concentrations systematically decrease in the downstream direction (Table 1). At Fischa-Dagnitz, where groundwater discharge occurs along the length of the stream, water at the spring orifices are probably not as well mixed as the stream water. Twenty-two tritium samples were collected at 18 locations; the mean tritium concentration (rounded) was 9.8 TU. The gas samples have small amounts of excess air, as indicated by delta-neon (ΔNe) ranging from 15 to 24%. Mean gas concentrations of ^{3}H, ^{4}He, and ^{84}Kr in groundwater at the nearby monitoring wells are 10.8 TU, 5.54 e-8 ccSTP/g, and 5.08 e-8 ccSTP/g, respectively (Table 1). The analytical error in gas and ^{3}H analysis is 1% and 3%, respectively.

[19] Stream discharge increases from 54 L/s at Fischa-Dagnitz spring (FS-1) to 679 L/s at the Grossmittler Road bridge, 1,899 m downstream (Figure 3). Stream discharges were measured at 12 locations (Table 2). Increased streamflow is due solely to groundwater inflow; there are no surface water tributaries along the study reach. Groundwater inflow along the upper 300 m of stream is about 1.5 L per

Table 1. Gas Concentration in Water Samples Collected at the Fischa-Dagnitz Stream and Nearby Monitoring Wells, Southern Vienna Basin, Austria, European Union

Sample Name	Location Number Used on Figure 1	Sampling Date	Distance Downstream (m)	N_2 (ccSTP/g)	^{40}Ar (ccSTP/g)	^{84}Kr (ccSTP/g)	^{20}Ne (ccSTP/g)	^{4}He (ccSTP/g)	^{3}He (ccSTP/g)	R/R_a[a]	Tritium (TU)
Samples Collected Prior to Gas Tracer Test or Above Injection Location											
Fischa Spring #1	FS	10/3/06	12	0.0159	4.14E-04	5.24E-08	1.91E-07	4.84E-08	7.16E-14	1.070	9.4
Fischa Spring #1[b]	FS	10/5/06	12	0.0178	4.03E-04	5.24E-08	1.89E-07	4.94E-08	7.31E-14	1.069	9.4
Fischa Spring #2	S #2	10/1/06	–	0.0163	4.36E-04	5.59E-08	2.06E-07	5.44E-08	9.28E-14	1.233	9.6
deadend spring	DE	10/1/06	–	0.0167	4.10E-04	5.41E-08	1.97E-07	4.81E-08	7.30E-14	1.098	9.9
F-200	F-3	10/1/06	181	0.0154	4.25E-04	5.25E-08	1.96E-07	5.15E-08	8.57E-14	1.201	9.9
F-700	F-12	10/1/06	652	0.0174	4.23E-04	5.27E-08	1.93E-07	4.94E-08	7.95E-14	1.163	10.0
F-900	F-14	10/1/06	838	0.0169	4.14E-04	5.44E-08	1.91E-07	4.85E-08	7.47E-14	1.114	9.8
F-1100	F-16	10/1/06	1030	0.0173	3.89E-04	5.04E-08	1.86E-07	4.61E-08	6.90E-14	1.081	9.5
F-1300	F-17	10/1/06	1229	0.0179	4.17E-04	5.19E-08	1.88E-07	4.74E-08	7.27E-14	1.108	9.7
Grossmittler Bridge	F-19	10/1/06	1887	0.0177	4.24E-04	5.40E-08	1.94E-07	4.77E-08	7.12E-14	1.078	9.7
Samples Collected During Gas Tracer Test[c]											
F-250	F-4	10/5/06	241	0.0181	4.19E-04	9.81E-08	2.01E-07	6.03E-08	8.31E-14	0.996	9.9
F-300	F-5	10/5/06	280	0.0180	4.25E-04	8.66E-08	1.99E-07	5.89E-08	8.58E-14	1.052	9.9
F-350	F-6	10/5/06	330	0.0162	4.23E-04	8.52E-08	1.99E-07	5.86E-08	8.22E-14	1.014	9.9
F-400	F-7	10/5/06	322	0.0171	4.16E-04	8.34E-08	1.99E-07	5.65E-08	8.00E-14	1.023	9.9
F-450	F-8	10/5/06	442	0.0162	4.50E-04	8.56E-08	2.11E-07	5.91E-08	8.66E-14	1.059	9.9
F-500	F-9	10/5/06	403	0.0166	4.16E-04	8.15E-08	1.99E-07	5.50E-08	8.02E-14	1.053	9.9
F-600	F-11	10/5/06	578	0.0149	4.27E-04	8.05E-08	2.03E-07	5.55E-08	8.19E-14	1.066	9.9
F-700	F-12	10/5/06	652	0.0150	4.14E-04	7.98E-08	1.99E-07	5.38E-08	7.93E-14	1.065	10.0
F-800	F-13	10/5/06	741	0.0164	4.04E-04	7.39E-08	1.89E-07	5.07E-08	7.07E-14	1.007	10.0
F-950	F-15	10/5/06	882	0.0179	4.14E-04	7.49E-08	1.93E-07	5.16E-08	7.39E-14	1.034	9.8
F-1100	F-16	10/5/06	1030	0.0180	4.08E-04	7.13E-08	1.90E-07	5.00E-08	7.18E-14	1.038	9.5
F-1300	F-17	10/5/06	1129	0.0171	4.01E-04	6.80E-08	1.84E-07	4.83E-08	6.98E-14	1.043	9.7
Samples Collected From Nearby Monitoring Wells											
Well F	W-3	10/6/06		0.0159	3.66E-04	4.77E-08	1.87E-07	4.59E-08	6.72E-14	1.057	10.5
Well 379	W-2	10/6/06		0.0182	4.09E-04	5.26E-08	2.20E-07	5.93E-08	1.05E-13	1.277	11.3
Well 233	W-1	10/6/06		0.0160	4.06E-04	5.27E-08	2.14E-07	5.68E-08	9.63E-14	1.225	11.0
Well TH2	W-4	10/6/06		0.0188	4.02E-04	5.02E-08	2.25E-07	5.95E-08	1.05E-13	1.280	10.5

[a]R is the ratio of $^{3}He/^{4}He$ in the water sample; R_a is the ratio of $^{3}He/^{4}He$ in air.
[b]Sample collected during the gas tracer test. Fischa Spring #1 is located about 180 m upstream of the gas injection point.
[c]Injection of Helium and Krypton.

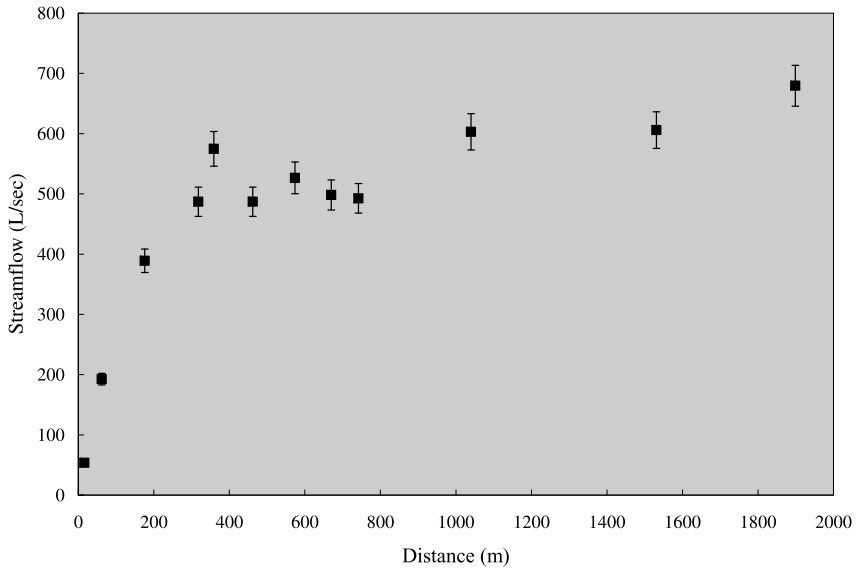

Figure 3. Graph showing stream discharge at various distances downstream from Fischa-Dagnitz spring.

Table 2. Stream Discharge Measurements for the Fischa-Dagnitz Stream, Southern Vienna Basin, Austria, European Union

Location Name	Location Number Used on Figure 1	Date	Distance Down Stream From Fischa Spring #1 (m)	Stream Width (m)	Mean Stream Depth (m)	Stream Cross-Sectional Area (m^2)	Mean Velocity of Stream Water (m/sec)	Stream Discharge (L/s)
F-12	F-1	9/29/06	16	2.5	0.17	0.43	0.13	54
F-100	F-2	9/30/06	62	2.8	0.28	0.78	0.25	193
F-200	F-3	9/30/06	176	3.9	0.30	1.17	0.33	389
F-325 (Pegel)	F-6	9/30/06	318	2.9	0.40	1.18	0.41	487
F-400	F-8	9/30/06	359	4.3	0.26	1.14	0.51	575
F-500	F-10	9/30/06	462	5.0	0.27	1.36	0.36	487
F-600	F-11	10/3/06	574	5.6	0.15	0.86	0.61	527
F-700	F-12	10/3/06	670	5.0	0.32	1.63	0.31	498
F-800	F-13	10/3/06	742	5.4	0.29	1.55	0.32	493
F-1100	F-16	10/6/06	1040	5.4	0.24	1.30	0.46	603
F-1550	F-18	10/6/06	1531	6.8	0.24	1.63	0.37	606
Grossmittler Bridge	F-19	10/3/06	1899	10.9	0.34	3.70	0.18	679

second per linear meter of streambed and accounts for about 70% of the total flow measured at the bridge. The remaining 30% of gains (0.12 L per second per linear meter of streambed) occurs along the lower 1600 m of stream. Discharge is typically assigned an accuracy based on the opinion of the individual making the measurement [*Wilberg and Stolp*, 2004]. Discharge measurements along the Fischa-Dagnitz stream were considered "good," which means an error of ±5%.

[20] Helium and Kr gas was injected for a period of 96 h at a location about 180 m downstream of Fischa-Dagnitz spring. Diffusion samplers were deployed within 4 h of the start of injection and collected 93 h after the start of injection. Twelve samples were collected and results are listed in Table 1. The ^{4}He concentration in stream water 61 m below the injection location was 6.03 e-8 ccSTP/g. This is 1.4 times above the air-equilibrated value of 4.5 e-8 ccSTP/g. Elevated ^{84}Kr was 9.81 e-8 ccSTP/g at 61 m, which is a factor of 2 above the air-equilibrated value (4.9 e-8 ccSTP/g). These concentrations indicate that effective diffusion coefficients for ^{4}He and ^{84}Kr are approximately 2.0 e-9 and 3.2 e-8 m^2/sec. Ideally some combination of longer tubing lengths (40 to 50 m) and/or higher injection system backpressure should have been used to achieve the desired concentrations of 1 order of magnitude above air equilibration.

5. Interpretations and Discussion

5.1. Gas Exchange Characteristics

[21] Gas exchange characteristics (λ and n) for Fischa-Dagnitz were quantified by calibrating the modified version of OTIS to the elevated values of ^{4}He and ^{84}Kr created during the gas tracer test. The calibration was done by setting C_{in} for ^{4}He and ^{84}Kr equal to the mean concentrations of the 4 monitoring wells. Ideally, gas concentrations would have been elevated to the point where simulation results were insensitive to C_{in} and dependent only on λ. At gas concentrations obtained during the tracer test (a factor of 2 or less), simulation results are dependent on both C_{in} and the measured change in gas concentration relative to distance below the gas injection location. Fixing C_{in} simplifies the calibration process but increases uncertainty associated with the derived λ's for ^{4}He and ^{84}Kr (Table 3). To determine λ's for ^{3}He and ^{20}Ne, equation (3) was used with n equal to 0.5 (see Appendix A2).

5.2. Groundwater Inflow Concentrations

[22] Once λ's for ^{3}He, ^{4}He, ^{20}Ne, and ^{84}Kr were established, the modified OTIS simulator was used to model C_{in}'s for each of the gases. The λ's values were fixed for each of the gases and the C_{in}'s adjusted to minimize the difference between simulated and measured (naturally occurring) gas concentrations in stream water. The C_{in}'s that result in minimum sigma values are listed in Table 3; comparison of measured and simulated stream water concentrations are shown in Figures 4 and 5. With the C_{in}'s listed in Table 3, the estimated inflow concentration of $^3He_{trit}$ is 8.3 TU. The $^3He_{trit}$ amount (^{3}He resulting from ^{3}H decay) was separated from total ^{3}He in the water sample by subtracting out atmospheric and terrigenic sources. The excess air portion of atmospheric ^{3}He was estimated using the CE model. The ^{3}H concentration, 9.8 TU, was calculated as the mean of 22 stream water samples. We consider these concentrations of $^3He_{trit}$ and ^{3}H to be reasonable estimates of the flow-weighted mean for groundwater discharging at Fischa-Dagnitz.

5.3. Transit Time Distribution

[23] A fundamental assumption of this paper is that C_{in}'s for $^3He_{trit}$ and ^{3}H are the most suitable values for estimating MTT of the aquifer contributing water to Fischa-Dagnitz. However, the flow-weighted mean $^3He_{trit}$ and ^{3}H concentrations were not translated to a mean apparent age using the standard age equation [*Schlosser et al.*, 1989]. Because the age equation is nonlinear, evaluating the equation using mean concentration (although flow weighted) does not map to the mean of the function (in this case the mean apparent age). Instead, a transit time distribution of the discharging groundwater was estimated and used to evaluate MTT. In most cases, data are not available to clearly define a transit time distribution; as a result, sources of recharge, water budgets, and recharge-discharge geometry need to be used to make a first-order estimate of the distribution. That type of broad-scale quantification often contains a large degree of uncertainty. The choice of transit time distribution can be constrained by vertical age profiling of the aquifer water (see Appendix A3).

Table 3. Parameters Used in One-Dimensional Transport With Inflow and Storage (OTIS) Simulations of Gas Exchange for the Fischa-Dagnitz Stream, and Gas Concentrations Used in the Closed System Equilibrium (CE) Model to Calculate Apparent Age, Southern Vienna Basin, Austria, European Union

Gas	Upstream Boundary Inflow (L/min)	Upstream Boundary Gas Concentration (ccSTP/g)	Air-Equilibration Concentration at 230 m and 11.2°C (ccSTP/g)	Groundwater Inflow Concentration, C_{in} (ccSTP/g)	Gas Exchange Coefficient Range, λ (1/s)	Aqueous Diffusion Coefficient at 11°C (cm^2/s)[a]	Gas Exchange Coefficient, λ (1/s)[b]
			OTIS Simulation of Gas Tracer Test[c]				
Helium-4 (^{4}He)	419[d]	6.03 e-8[d]	4.5 e-8[d]	5.54 e-8[d]	4.9 to 5.8 e-4[e]	5.80 e-5	5.8 e-4
Krypton-84 (^{84}Kr)	419[d]	9.81 e-8[d]	4.9 e-8[d]	5.08 e-8[d]	2.7 to 3.6 e-4[e]	1.24 e-5	2.7 e-4
Helium-3 (^{3}He)	not simulated	not simulated	not simulated	not simulated	not simulated	6.67 e-5[f]	6.2 e-4
Neon-20 (^{20}Ne)	not simulated	not simulated	not simulated	not simulated	not simulated	3.07 e-5	4.2 e-4
			OTIS Simulation of Natural Conditions[g]				
Helium-3 (^{3}He)	0[d]	7.25 e-14[d]	6.2 e-14[d,h]	9.7 e-14[e]			same as above
Helium-4 (^{4}He)	0[d]	4.89 e-8[d]	4.5 e-8[d]	5.3 e-8[e]			same as above
Neon-20 (^{20}Ne)	0[d]	1.90 e-7[d]	1.8 e-7[d]	2.1 e-7[e]			same as above
Krypton-84 (^{84}Kr)	0[d]	5.24 e-8[d]	4.9 e-8[d]	5.5 e-8[e]			same as above
			CE Simulation[i]				
Helium-3 (^{3}He)				9.7 e-14			
Helium-4 (^{4}He)				5.3 e-8			
Neon-20 (^{20}Ne)				2.1 e-7			
Krypton-84 (^{84}Kr)				5.5 e-8			
Tritiogenic helium-3 (^{3}He$_{trit}$)				2.1 e-14[j]			

[a]Diffusion coefficients modified from *Cook and Herczeg* [2000, Appendix 4] using the temperature correction formulation from *Jähne et al.* [1987].
[b]Determined using equation (3) and n = 0.5.
[c]OTIS simulations of the gas tracer test were done to determine gas exchange coefficients.
[d]Fixed parameters.
[e]Calibration parameters.
[f]Calculated as D_{4He} * 1.15; [*Jähne et al.*, 1987].
[g]OTIS simulations of natural conditions were done to determine gas concentrations of inflowing groundwater.
[h]Calculated as ^{4}He * R_a; R_a = 1.384 e-6.
[i]CE simulation was done to determine the atmospheric excess-air component of helium-3 of inflowing groundwater.
[j]Equivalent to 8.3 TU.

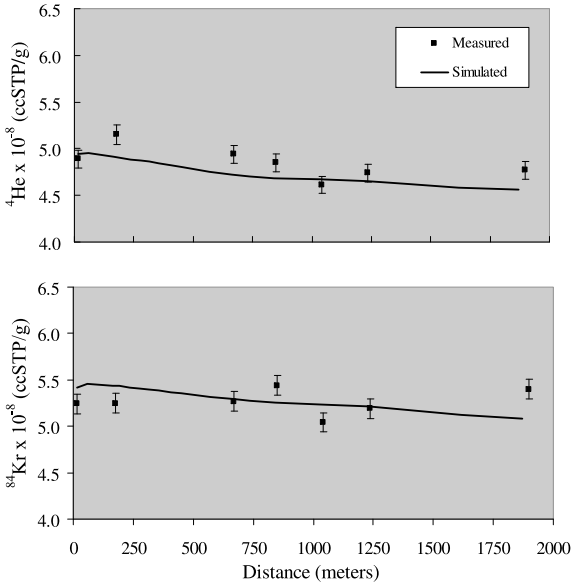

Figure 4. Measured and simulated ^{4}He and ^{84}Kr values in stream water, Fischa-Dagnitz system.

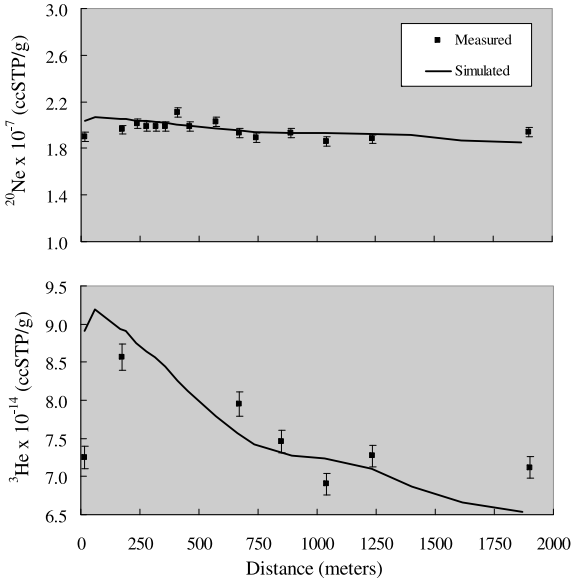

Figure 5. Measured and simulated ^{20}Ne and ^{3}He concentrations in stream water, Fischa-Dagnitz system.

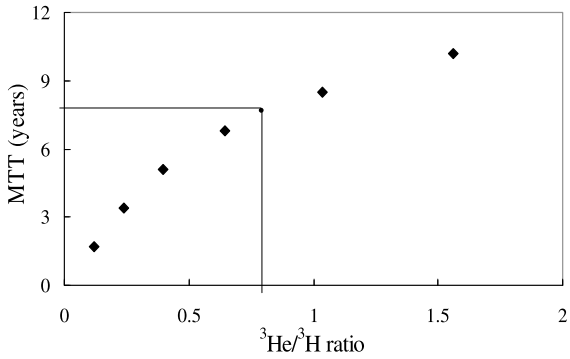

Figure 6. The $^3He_{trit}$-^3H ratio derived from the hybrid age model for a range of MTT's.

[24] For Fischa-Dagnitz, the primary source of recharge (approximated at 70%) is conceptualized as coming from the Schwarza River; the remaining recharge is estimated to originate from precipitation and irrigation. Discharge is at the springs and emerging stream. The transit time distribution for groundwater originating at the Schwarza River should be reasonably well represented by a dispersion model; precipitation and irrigation result in an exponential age structure [*Cook and Böhlke*, 2000]. This concept of aquifer recharge results in a hybrid dispersion-exponential distribution of transit times at the springs and emerging stream. Parameters of the hybrid age model are the exponential and dispersion MTTs, a dispersion parameter (P_d) [*Kreft and Zuber*, 1978], and the mixing ratio between the two models. Details of the hybrid age model are given in Appendix A4.

5.4. Mean Transit Time

[25] To characterize a MTT for Fischa-Dagnitz from the flow-weighted $^3He_{trit}$–^3H concentrations, the hybrid age model was run for MTTs that range from 1 to 20 years. For each simulated MTT the hybrid model outputs corresponding $^3He_{trit}$ and ^3H concentrations for 2006, the year for which flow-weighted mean concentrations were estimated. The MTT and corresponding $^3He_{trit}$–^3H ratios for 2006 are plotted on Figure 6. Hybrid age model output was calculated using FlowPC [*Maloszewski and Zuber*, 1996] using average annual ^3H concentration in precipitation at Gloggnitz, Austria (Figure 7) as input.

[26] The hybrid age model parameters were constrained by scaling the dispersion and exponential components of flow by 0.7 and 0.3, respectively. Mean transit times of the dispersion and exponential components were fixed at a ratio of 2:1, to maintain traveltime consistency. This ratio reflects the 20 km flow-path length of groundwater originating from the Schwarza River, and the 10 km average flow-path length of groundwater recharged across the spatial extent of the contributing aquifer. The simulated $^3He_{trit}$–^3H concentration ratio for 2006 is comparable to the estimated ratio (8.3 TU/9.8 TU = 0.85) for a MTT of 8 years (Figure 6). Using flow-weighted and exchange-corrected gas con-

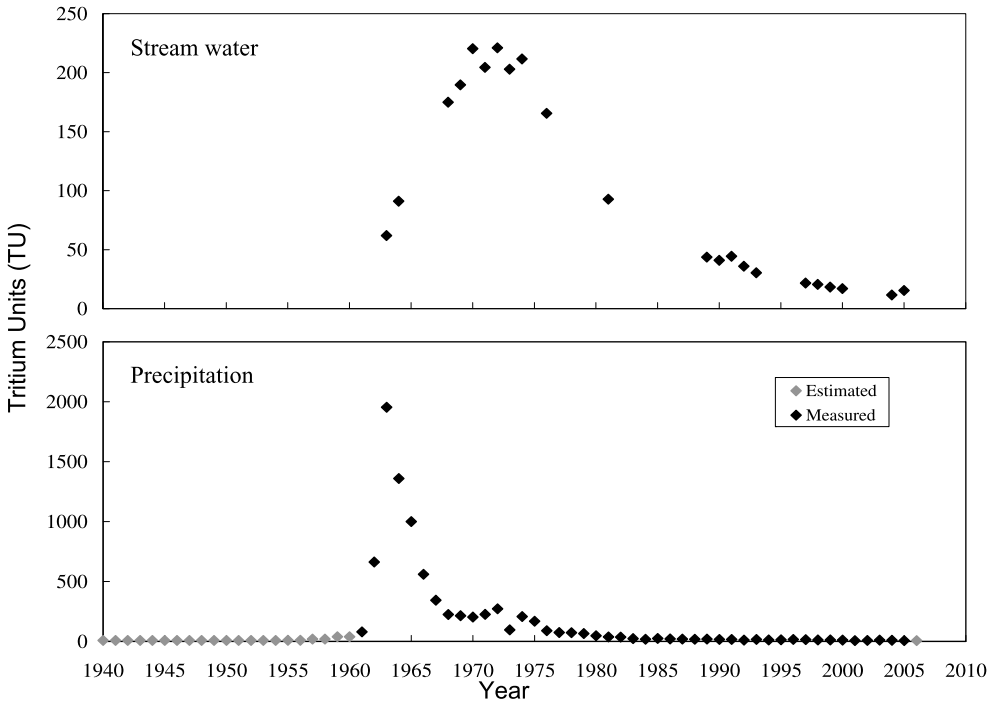

Figure 7. Time series of tritium in stream water of the Fischa-Dagnitz system, and tritium in precipitation at Gloggnitz, Austria.

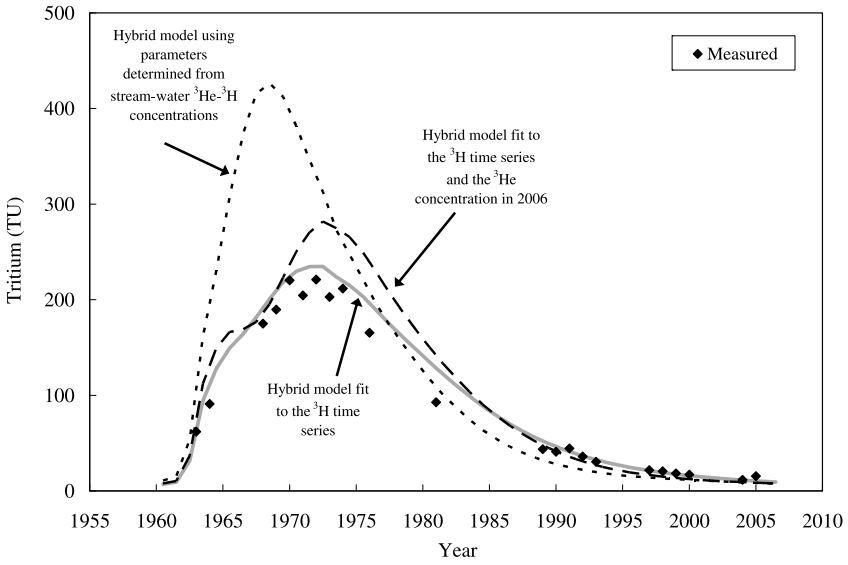

Figure 8. Results from the hybrid age model simulations.

centrations, 8 years is the best estimate of MTT for the contributing aquifer.

6. Method Verification Using the Measured ^{3}H Time Series

[27] A long-term time series of ^{3}H concentrations in stream water at Fischa-Dagnitz makes it possible to independently assess transit times and compare to MTT derived from stream water $^3He_{trit}$–^{3}H. Analysis of the ^{3}H time series was done using the same hybrid age model outlined in the previous section and detailed in Appendix A4.

[28] When the 8 year MTT derived from fitting the estimated 2006 stream water $^3He_{trit}$–^{3}H ratio is used to model ^{3}H, simulated values exceed measured values by a factor of 2 (Figure 8). The simulated ^{3}H peak occurs in 1966; the measured peak occurs between 1970 and 1974. The shape and timing of the simulated peak is set by the short MTT and modest dispersion (Table 4). The measured and simulated ^{3}H time series are nearly identical when the composite MTT is increased to 14 years, but simulated $^3He_{trit}$ for 2006 is a factor of 3 greater than the estimated amount of 8.3 TU (Table 4). Increasing MTT broadens the transit time distribution which in turn causes $^3He_{trit}$ derived from the bomb-peak to be incorporated into the total simulated for 2006. There are several likely reasons for the difference between estimated and simulated $^3He_{trit}$. The first is diffusive loss of ^{3}He across the water table (see Appendix A5), which will cause a decrease in measured values in stream water. Another reason may be that gas exchange across the air-

Table 4. Parameters Used in FlowPC Simulations of the Tritium Output Time Series for the Fischa-Dagnitz Stream, Southern Vienna Basin, Austria, European Union

	Model Parameters						Results[a]			
		Dispersion Component			Exponential Component					
Model Option	Composite MTT (years, rounded)	MTT (years)	P_d	Fraction	MTT (years)	Fraction	Sigma[b] (TU)	^{3}H in 2006[c] (TU)	Tritiogenic ^{3}He in 2006[d] (TU)	Tritiogenic ^{3}He-^{3}H ratio[e] (unitless)
Hybrid model using parameters determined from stream-derived $^3He_{trit}$-^{3}H concentrations	8	9	0.2	0.7	4.5	0.3	not applicable	7.6	6	0.79
Hybrid model fit to the ^{3}H time series	14	16	0.2	0.7	8	0.3	3.7	9.2	25.5	2.77
Hybrid model fit to the ^{3}H time series and the ^{3}He concentration in 2006	11	13	0.1	0.7	6.5	0.3	7.4	7.8	10	1.28

[a]Tritium half-life used in calculations is 12.32 years.
[b]Based on the difference between measured and simulated ^{3}H concentrations for Fischa-Dagnitz stream water (see equation (2)).
[c]Measured value of ^{3}H in stream water at Fischa-Dagnitz is 9.8 TU.
[d]Estimated value of $^3He_{trit}$ of inflowing groundwater at Fischa-Dagnitz is 8.3 TU.
[e]Estimated tritiogenic ^{3}He - ^{3}H ratio at Fischa-Dagnitz is 0.85.

water interface is more rapid than estimated by λ and the applied correction is not correct. The most likely reason is that the transit time distribution (i.e., the hybrid age model) does not properly characterize all transport mechanisms within the contributing aquifer.

[29] Using a MTT of 11 years and a $P_d = 0.1$, the simulated 2006 $^3He_{trit}$ is reduced to 10 TU; however the simulated ^3H peak exceeds the measured peak by about 55 TU. The simulated ^3H peak occurs in 1973, which is reasonably close to the measured 1970–74 peak (Figure 8 and Table 4). The hybrid age model with an 11 year MTT represents a compromise that allows for an "acceptable" level of misfit between the simulated and measured ^3H time series, and $^3He_{trit}$ in 2006.

7. Concluding Remarks

[30] The methodology developed at Fischa-Dagnitz, though not without intricacies, is a reasonable approach to quantifying MTT. To summarize, estimates of gas exchange and groundwater inflow are used to simulate gas transport in the stream, and ultimately determine the flow-weighted groundwater inflow concentrations of $^3He_{trit}$. In combination with measured stream water ^3H concentrations, and using a conceptually based estimate of the age structure in the aquifer, a MTT of the contributing aquifer was quantified.

[31] It was clear from the onset that conditions at Fischa-Dagnitz are favorable for determining groundwater inflow concentrations. Groundwater inflow along the stream is on the order of 1 L per second per linear meter of streambed, suggesting that stream water concentrations probably require minimal correction for gas exchange.

[32] Once the inflowing groundwater concentration of $^3He_{trit}$ was determined, a distribution of transit times for the contributing aquifer was established on the basis of known and estimated recharge sources. Using the transit time distribution, the $^3He_{trit}$–^3He concentrations were used to estimate an 8 year MTT for the contributing aquifer. For conditions at gaining streams and springs, where water is well mixed and the distribution of transit times is expected to be broad, application of the standard age equation does not yield a meaningful estimate of MTT. This is due to the nonlinear nature of the age equation.

[33] The 8 year MTT estimate derived from gas-exchange corrected concentrations compares to the 14 year MTT that best describes the ^3H time series data that exists for Fischa-Dagnitz. Considering both ^3H time series data and estimated $^3He_{trit}$ concentration in 2006, the 11 year MTT results in an acceptable misfit between simulated and measured values. The misfit illustrates inherent uncertainty associated with estimating transit time distributions of heterogeneous natural systems. Accepting a worst-case error (where 14 years is the "true" MTT), the 8 year gas-exchange corrected MTT still provides a valuable constraint on fluid flow and storage volume within the contributing aquifer. Overall, the methods presented in this paper should be tested at other springs and gaining streams to fully determine utility and value.

Appendix A

A1. Method Applicability

[34] The chance of successfully sampling stream water such that the measured ^3He can be corrected to a groundwater inflow concentration depends on the amount of inflowing groundwater and gas-exchange at the air-water interface. Groundwater inflow to the stream transports ^3He above solubility equilibrium into the stream system while gas exchange transports ^3He out of the stream system. When inflow is large relative to gas-exchange, groundwater gas concentrations are preserved in the stream, and the possibility of successfully correcting for gas exchange and deriving representative C_{in}'s is good.

[35] The physical processes of inflow and exchange can be described as the ratio of the gas exchange velocity (k) to specific discharge (q). The gas exchange velocity is the product of λ and average stream depth [*Wanninkhof et al.*, 1990]; specific discharge is the measured groundwater inflow divided by the streambed area (stream length times width). Rapid gas exchange and small amounts of groundwater inflow results in large k/q values whereas slow exchange and large inflow result in small k/q values. In streams where k/q is small, the methods described in this paper can be applied.

[36] This concept is illustrated in Figure A1 where groundwater concentrations (normalized to the air-equilibrated concentration) and resulting stream water concentration (also normalized) as a function of gas transport are graphed. The k/q lines in Figure A1 where generated using OTIS with spatially constant values for k and q; this approach is a simplification that does not account for changes in stream width and depth caused by increased stream flow. Steady state conditions were simulated; this means the mass inflow of tracer gas from groundwater is matched by the mass outflow of gas due to exchange with the atmosphere. Groundwater inflow rates for the upper reach of Fischa-Dagnitz stream and the λ for ^3He (Figure 3 and Tables 2 and 3) results in a k/q equal to about 1. For the lower reach (284 to 1,899 m) where groundwater inflow is less, k/q equals 22. Comparisons on Figure A1 shows that when k/q is equal to 1, and the concentration of inflowing groundwater is twice the air-equilibrated concentration (C_{in}/C_{atm} is 2.0 on the x axis), the stream concentration (C_{stream}) is 1.87 times more then the air-equilibrated concentration. This means that if C_{in} is 12.4 e-14 ccSTP/g (twice the air-equilibrated value), stream concentration would be 11.5 e-14 ccSTP/g. The exchange correction required to recover the groundwater signal is relatively minor. When k/q becomes larger, the correction also becomes larger. For a k/q = 20, C_{stream}/C_{atm} is 1.38 when C_{in}/C_{atm} is 2.0; a 12.4 e-14 ccSTP/g groundwater signal would appear as a stream concentration of 8.6 e-14 ccSTP/g. When the exchange correction is larger the associated uncertainty also becomes larger. In this way the k/q ratio is an indirect qualifier of uncertainty. As k/q becomes larger the error associated with exchange-corrected gas signals also becomes larger. The methods discussed in the paper are more reliable when k/q is smaller.

[37] Because k/q describes the likelihood of successfully quantifying the gas concentration of inflowing groundwater, the ratio should be used as an initial screening tool. If stream conditions indicate that k/q > 20, the gas signal will be largely lost to the atmosphere. For Fischa-Dagnitz, the ^3He signal is preserved because of large groundwater inflows along the upper stream reach. Also implied by the k/q ratio is that for age tracers with smaller k values (e.g., due to lower diffusion coefficients, for example CFCs or ^{85}Kr) age

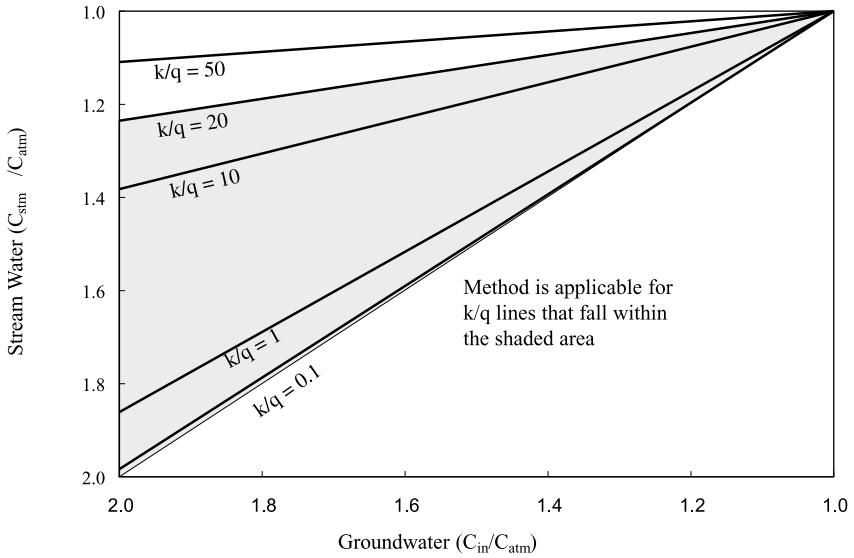

Figure A1. The relationship between the concentration of a volatile tracer (e.g., ^{3}He) in groundwater and stream water as a function of stream gas transport. The value k is the gas exchange velocity (L/t) and q is the specific discharge of groundwater into the stream.

information could be preserved along stream reaches with lesser amounts of groundwater inflow.

A2. Gas Exchange

[38] To correct for gas exchange across the air-water interface, λ's for ^{3}He, ^{4}He, ^{20}Ne, and ^{84}Kr need to be quantified. A probable range of λ values for both ^{4}He and ^{84}Kr were determined by injecting He and Kr into stream water and simulating gas transport. Using temperature corrected-diffusion coefficients for ^{4}He and ^{84}Kr (Table 3), and the corresponding λ ranges, equation (3) was solved for n. The combination of λ's that gives a value of n within the prescribed limit of 0.5 to 1.0 are 5.8 e-4/sec and 2.7 e-4/sec for ^{4}He and ^{84}Kr, respectively (Table 3). The value of n is 0.51. The value is at the lower-prescribed limit (n = 0.5) and implies turbulent flow as the only gas-exchange mechanism at Fischa-Dagnitz. Imposing n at the lower limit is not ideal and increases the level of uncertainty already associated with λ values. Despite these limitations, equation (3) was also used to derive λ values for ^{3}He and ^{20}Ne (no gas tracer test was conducted for ^{3}He and ^{20}Ne). The diffusion coefficient used for ^{3}He is 1.15 times more than the ^{4}He coefficient [*Jähne et al.*, 1987]. The λ values for ^{3}He and ^{20}Ne, imposing the n = 0.51 constraint, are 6.2 e-4/sec and 4.2 e-4/sec.

A3. Vertical Age Profiling

[39] Collecting and dating water from discrete flow paths at a fixed horizontal location can help to better define the age distribution that exists within the contributing aquifer. Discrete sampling can be done by constructing a nested set of monitoring wells that are open to progressively deeper intervals of the aquifer. The goal is to obtain discrete samples that represent a minimal number of flow paths. Figure A2 shows generalized vertical age profiles invoked by various age models. Each profile of age as a function of depth is distinct and can therefore be used to constrain the choice of age model used to estimate a MTT.

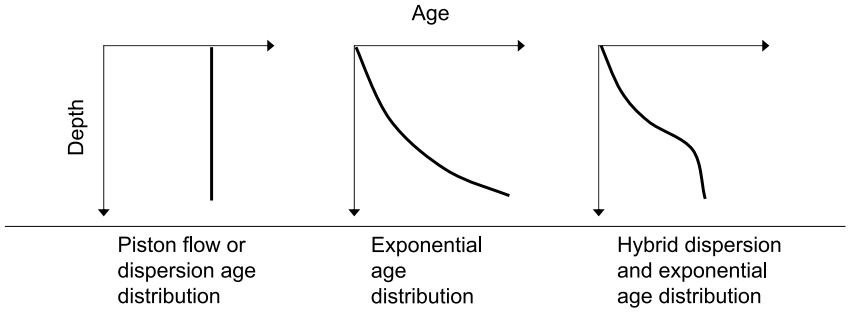

Figure A2. Generalized diagram of vertical age profiles for various age distributions within an aquifer.

A4. Transit Time Distribution

[40] Recharge sources for Fischa-Dagnitz are based on known areas of river infiltration, land use, and climatic conditions. Previous work identified significant groundwater recharge from the Schwarza River and essentially no spatially distributed recharge due to precipitation and irrigation [*Rank and Papesch*, 2003]. For the transit time distribution used in this analysis, irrigation and precipitation (which averages about 65 cm/yr) were considered sources of groundwater recharge to the contributing aquifer. Total recharge is considered equal to the measured stream discharge at Grossmittler Road (679 L/s).

[41] The amount of spatially distributed recharge was calculated using the surface expression of the contributing area, and an infiltration rate of 10%. Longitudinal length of the contributing area is defined by the distance to the Schwarza River (20 km). Transverse length is based on distances to the Piesting and Leitha Rivers, which are located about 5 km to the northwest and southeast of Fischa-Dagnitz, respectively (Figure 1). The two rivers and Fischa-Dagnitz likely create a series of groundwater divides that are assumed to evenly split the distances between them. This idealized situation would limit the traverse extent of the Fischa-Dagnitz contributing area to roughly 5 km (2.5 km to the northwest and 2.5 km to the southeast) and the total surface expression to 100 km^2. Using the 10% infiltration rate, the total amount of spatial recharge is about 200 L/sec, which is roughly 30% of measured discharge at Grossmittler Road. The remaining 70% of recharge is attributed to losses from the Schwarza River.

[42] Using this proportion, the hybrid age model was constrained by weighting flow of the dispersion and exponential components by 0.7 and 0.3, respectively. The hybrid age model was additionally constrained to maintain internal traveltime consistency by fixing the ratio of MTT for the dispersion and exponential components at 2:1. The ratio is based on flow path lengths. For the dispersion component the length is 20 km. For the exponential component the average length is estimated at 10 km. This represents a simplified average that assumes an even spatial distribution and is based on the longest dimension of the contributing area. Fixing the MTT ratio prevents simulating an exponential MTT that is greater than the dispersion MTT. The dispersion parameter P_d was fixed at 0.2, which creates a moderate amount of dispersion. The transit time distribution output (^3H and $^3He_{trit}$ concentrations for 2006) was computed using FlowPC with the dispersion model (DM) and exponential model (EM) options [*Maloszewski and Zuber*, 1996]. FlowPC does not include a hybrid EM/DM option; results were obtained by postprocessing (weighting and summing) results of individual DM and EM simulations.

A5. Diffusive Loss of ^3He

[43] When analyzing well-mixed spring/stream water that originates from an unconfined aquifer, the effects of gas loss due to diffusion across the water table should be considered. The loss of ^3He, and therefore $^3He_{trit}$, will result in apparent age estimates that are younger than the actual ages. The loss can be estimated using the characteristic diffusion length:

$$z = \sqrt{4D_{^3He}t} \qquad \text{(A1)}$$

where z is the distance below the water table at which the ^3He concentration would be 16% of air-equilibrated concentration, D is the aqueous diffusion coefficient for ^3He, and t is time. With D = 6.67 e-9 m^2/sec and t = 10 yr, diffusive losses of more than 16% of ^3He would only affect the upper 1 to 2 m of the aquifer. In the case of Fischa-Dagnitz, where the contributing aquifer is approximately 100 m thick, diffusive loss of ^3He is not considered significant. If aquifer thickness is on the order of 10 to 30 m, or the sample represents only water from the upper portions of an unconfined aquifer, the effects of diffusive loss may need to be accounted for.

[44] **Acknowledgments.** The authors gratefully acknowledge financial support of this work through award EAR-0309212 from the Hydrologic Sciences Program of the U.S. National Science Foundation, and logistical/analytical assistance from the International Atomic Energy Agency Isotope Hydrology Section, especially Manfred Groening. Three anonymous peer reviewers improved technical soundness, particularly the deviation between apparent age and MTT. The authors thank Rob Runkel of the U.S. Geological Survey for modifying OTIS to simulate gas transport and Lawrence Spangler of the U.S. Geological Survey for editorial assistance.

References

Aeschbach-Hertig, W., F. Peeters, U. Beyerle, and R. Kipfer (2000), Paleotemperature reconstruction from noble gases in ground water taking into account equilibration with entrapped air, *Nature*, *405*, 1040–1044, doi:10.1038/35016542.

Busenberg, W., and L. N. Plummer (1992), Use of chlorofluorocarbons (CCl_3F and CCl_2F_2) as hydrologic tracer and age-dating tools: The alluvium and terrace system of Central Oklahoma, *Water Resour. Res.*, *28*, 2257–2283, doi:10.1029/92WR01263.

Cook, P. G., and J. K. Böhlke (2000), Determining the timescales for groundwater flow and solute transport, in *Environmental Tracers in Subsurface Hydrology*, edited by P. G. Cook and A. L. Herczeg, pp. 1–30, Kluwer Acad., Boston, Mass.

Cook, P.G., and A. L. Herczeg (2000), Environmental tracers in subsurface hydrology, Kluwer Acad. Publ., Boston, Mass.

Cook, P. G., and D. K. Solomon (1997), Recent advances in dating young groundwater: Chlorofluorocarbons, $^3H/^3He$ and ^{85}Kr, *J. Hydrol.*, *191*, 245–265, doi:10.1016/S0022-1694(96)03051-X.

Dincer, T., A. Al-Mugrin, and U. Zimmermann (1974), Study of the infiltration and recharge through the sand dunes in arid zones with special reference to the stable isotopes and thermonuclear tritium, *J. Hydrol.*, *23*, 79–109, doi:10.1016/0022-1694(74)90025-0.

Haitjema, H. M. (1995), On the residence time distribution in idealized groundwatersheds, *J. Hydrol.*, *172*, 127–146, doi:10.1016/0022-1694(95)02732-5.

Jähne, B., G. Heinz, and W. Deitrich (1987), Measurement of the diffusion coefficients of sparingly soluble gases in water, *J. Geophys. Res.*, *92*, 10,767–10,776, doi:10.1029/JC092iC10p10767.

Kazemi, G. A., J. H. Lehr, and P. Perrochet (2006), *Groundwater Age*, John Wiley, Hoboken, N. J., doi:10.1002/0471929514.

Kreft, A., and A. Zuber (1978), On the physical meaning of the dispersion equation and its solutions for different initial and boundary conditions, *Chem. Eng. Sci.*, *33*, 1471–1480.

Maloszewski, P., and A. Zuber (1996), Lumped parameter models for interpretation of environmental tracer data, in *Manual on Mathematical Models in Isotope Hydrology*, *Rep. IAEA-TECDOC 910*, pp. 9–58, Intl. At. Energy Agency, Vienna.

McGuire, K. J., and J. J. McDonnell (2006), A review and evaluation of catchment transit time modeling, *J. Hydrol.*, *330*, 543–563, doi:10.1016/j.jhydrol.2006.04.020.

Rank, D., and W. Papesch (2003), Determination of groundwater flow velocity in the Southern Vienna Basin from long-term environmental isotope records, in *Abstract Volume of the First Conference on Applied Environmental Geology in Central and Eastern Europe: BE-228*, edited by M. Kralik, H. Haeusler, and C. Kolesar, pp. 206–207, Umweltbundesamt, Vienna.

Runkel, R. L. (1998), One dimensional transport with inflow and storage (OTIS): A solute transport model for streams and rivers, *U.S. Geol. Surv. Water Resour. Invest. Rep.*, *98–4018*, 73 p.

Schlosser, P., M. Stute, C. Sonntag, and K. O. Münnich (1989), Tritiogenic ^{3}He in shallow groundwater, *Earth Planet. Sci. Lett.*, *94*(3–4), 245–256, doi:10.1016/0012-821X(89)90144-1.

Solomon, D. K., and P. G. Cook (2000), ^{3}H and ^{3}He, in *Environmental Tracers in Subsurface Hydrology*, edited by P. G. Cook and A. L. Herczeg, pp. 397–424, Kluwer Acad., Boston, Mass.

Wanninkhof, R., P. J. Mulholland, and J. W. Elwood (1990), Gas exchange rates for a first-order stream determined with deliberate and natural tracers, *Water Resour. Res.*, *26*, 1621–1630.

Wilberg, D. E., and B. J. Stolp (2004), Seepage investigation and selected hydrologic data for the Escalante River drainage basin: Garfield and Kane Counties, Utah, 1909–2002, *U.S. Geol. Surv. Sci. Invest. Rep.*, *2004–5233*, 39 p.

P. K. Aggarwal, L. F. Han, A. Suckow, and T. Vitvar, Isotope Hydrology Section, International Atomic Energy Agency, Wagramerstrasse 5, Vienna A-1400, Austria.

D. Rank, Center for Earth Sciences, University of Vienna, Althanstrasse 14, Vienna A-1090, Austria.

D. K. Solomon and B. J. Stolp, Geology and Geophysics Department, University of Utah, Salt Lake City, UT 84112, USA. (bjstolp@usgs.gov)

CHAPTER 5

CONCLUSIONS

The three components of work presented in this dissertation point out 1) the importance of understanding the basic hydrology of the stream or spring that is being sampled to determine mean transit time, 2) with favorable conditions, the non-conservative nature of age-dating environmental tracers can be mitigated, and 3) with careful measurement and interpretation, the original premise of being able to quantify a mean transit time at springs and gaining streams, is possible. The described methodology holds the potential that with a limited investment of time, effort, and fairly simple field instrumentation and infrastructure, mean transit time of water resources can be obtained. The information can then be used in conjunction with existing anecdotal and measured data to make 1st order estimates of water resource stability, sensitivity, permanence, and resilience. This could be of most value in developing countries where historic records and rigorous quantification of water resources may not exist.

Several additional areas of research would be useful to further develop mean transit time investigations. The most important would be testing the concept of an inverse correlation between streamflow variability and mean transit time. Does a stream with greater annual variations in baseflow represent a drainage basin with less groundwater storage shorter mean transit times? This could be done by estimating mean transit time, by the described methods, at a number of preselected drainage basins with a broad range

of streamflow variability. Variability would be identified from existing streamflow records.

Another valuable research area would be testing and developing more robust methods of estimating the transit time distribution. The distribution of groundwater age reveals information on the spatial distribution of recharge within a contributing area, which is also a powerful description of the water resource. This could be done using shallow piezometers to longitudinally and vertically profile a converging flowfield, which occurs at springs and gaining streams, the same types of areas discussed in this dissertation. Both discharge and piezometer water would be sampled for a suite of age-dating environmental tracers. In complement, the discharging groundwater would be continuously monitored for temperature, specific conductance, and discharge. These investigations should be conducted for basins that have been previously described with a calibrated numerical groundwater flow model. The model could then be used to simulate tracer transport to the discharge area. Deconvolving the mixed samples is the opposite of the techniques described in this paper that measure mixed sample to determine a mean transit time. Using the opposite technique would be an important contrast to derived values of mean transit time. The distributions of ages will also further understanding of the mixing process and the influence of young verses old groundwater.

A third area of interest is how the environmental tracers used in this study could be used to delineate groundwater inflow to larger volume streams where injected tracer or successive velocity discharge measurement techniques may not be viable. In this case the nonconservative nature of the tracers becomes advantageous. Where groundwater inflow occurs, the tracer signature would be exhibited in terms of concentrations that are not at

air-equilibration values. With distance downstream from groundwater inflow, where the stream may be neutral or losing, the tracer signature would dissipate to the air equilibration value. The disadvantage is that inflows that are small relative to streamflow might evoke so little concentration change that it cannot be measured. The advantage of using the tracers is that they can be measured with a high level of accuracy and the background concentration will always trend toward the known air-equilibration concentration.